Journal of Petroleum Science and Engineering 218 (2022) 111049

Contents lists available at ScienceDirect

Journal of Petroleum Science and Engineering

journal homepage: www.elsevier.com/locate/petrol

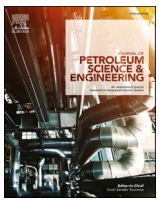

A new method for characterizing dynamic reservoir quality: Implications for quality maps in reservoir simulation and rock type classification

Abouzar Mirzaei-Paiaman [a,*], Behzad Ghanbarian [b]

[a] University of Campinas (UNICAMP), Campinas, SP, Brazil
[b] Porous Media Research Lab, Department of Geology, Kansas State University, Manhattan, 66506, KS, USA

ARTICLE INFO

Keywords:
Reservoir rock quality
DRQI
TEM-Function
Relative permeability
Rock typing
Quality map

ABSTRACT

Determining reservoir quality is vital in order to efficiently produce hydrocarbon and/or inject fluids for secondary/tertiary recovery and carbon sequestration. In this study, we introduce a new approach and present dynamic reservoir quality index (DRQI). A high-quality reservoir would have high displacement (recovery) rate and displaceable (recoverable) saturation of oil. A modified true effective mobility (TEM) function is developed representing displacement rate of oil by an injected fluid (e.g., water or CO_2). DRQI is defined as the area under modified TEM curve of oil and includes the well-known reservoir quality index (RQI) as its special case. A large dataset composed of 220 water displacing oil relative permeability experiments, conducted on limestone and dolomite rocks from three Iranian carbonate reservoirs, was used to investigate the potential relationships between DRQI and other reservoir characteristics (e.g., irreducible water saturation, bulk irreducible water, maximum movable oil saturation, and bulk maximum movable oil) as well as quality indicators of RQI, flow zone indicator (FZI), and Winland r35. Results showed that irreducible water saturation and maximum movable oil saturation as well as their bulk variants may not be appropriate for characterizing multiphase quality of reservoirs. Furthermore, the frequently-used single-phase rock quality indicators RQI, FZI, and Winland r35 were not found to be very accurate in characterization of dynamic reservoir quality. DRQI can be used in reservoir simulation studies as a criterion for defining quality maps, and in petrophysical tasks for rock typing and comparing between dynamic qualities (in terms of displacement rate and displaceable saturation of oil) of rock samples.

1. Introduction

Reservoir quality is a general term whose definition depends on the goals of a study. Here, we focus on quality in the context of multiphase flow, such as CO_2 injection into geological formations, aquifer rise, gas-cap expansion, and secondary and tertiary recovery processes. Understanding the distribution of rock quality is economically important for successful production and injection strategies (Nakajima and Schiozer, 2003; da Cruz et al., 2004).

Several approaches exist for assessing reservoir quality, such as petrographic studies (Nabawy, 2013; Tavakoli, 2018, 2021), analysis of well logging and seismic attributes (Ozkan et al., 2011; Nabawy and El Sharawy, 2018; Abdulaziz et al., 2019), use of routine core analysis data (Amaefule et al., 1993; Mirzaei-Paiaman et al., 2015, 2018), and analysis of special core analysis measurements like capillary pressure and relative permeability data (Skalinski et al., 2014; Chandra et al., 2015; Mirzaei-Paiaman et al., 2019b; Mirzaei-Paiaman and Ghanbarian, 2021a). Petrographic studies based on thin section images may provide some general qualitative and case-specific relations between pore-level quality and porosity or permeability (Nazari et al., 2019). However, the interrelation between pore-scale features and displacement rate and sweep efficiency is not yet fully known. In addition to that, thin sections only provide 2D images of a rock sample and do not capture heterogeneity in the third dimension.

The ratio of permeability (k) to porosity (φ) has been used as a quality indicator in scaling capillary pressure data through the well-known J-function (Leverett, 1941) and to characterize layer-scale quality (called process or delivery speed) (Chopra, 1988; Chopra et al., 1989). Amaefule et al. (1993) called this ratio reservoir quality index (RQI).

* Corresponding author.
E-mail address: Mirzaei1986@gmail.com (A. Mirzaei-Paiaman).

https://doi.org/10.1016/j.petrol.2022.111049
Received 20 April 2022; Received in revised form 29 August 2022; Accepted 9 September 2022
Available online 15 September 2022

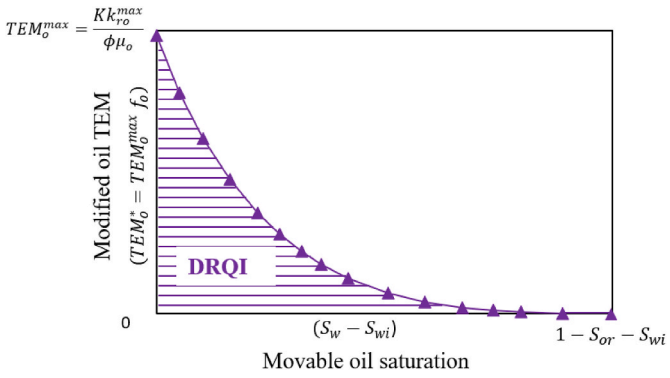

Fig. 1. Modified oil TEM, Eq. (7), against movable oil saturation. The area below the curve represents the DRQI, Eq. (8) or (9).

$$RQI = 0.0314\sqrt{\frac{k}{\varphi}} \tag{1}$$

in which permeability, porosity, and RQI are respectively in millidarcies, fraction, and micrometers. Since RQI is determined from single-phase flow characteristics (e.g., porosity and permeability), it should not be used to characterize the dynamic behavior of rocks under multiphase flow conditions.

To identify hydraulic flow units (HFUs), Amaefule et al. (1993) modified Kozeny-Carman equation and introduced flow zone indicator (FZI) as follows

$$FZI = 0.0314\frac{1-\varphi}{\varphi}\sqrt{\frac{k}{\varphi}} \tag{2}$$

where FZI is in micrometers. Similar to RQI, FZI does not consider multiphase characteristics. In addition to that, Mirzaei-Paiaman et al. (2015, 2018) argued that FZI is not a reliable HFU indicator and

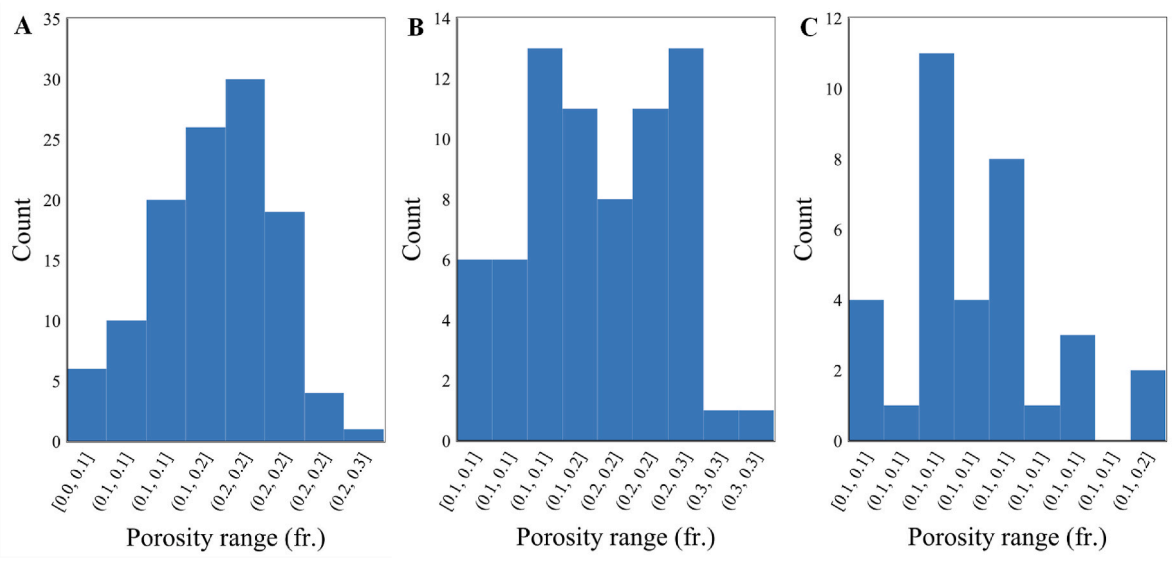

Fig. 2. Porosity histogram for samples from (A) Reservoir A, (B) Reservoir B, and (C) Reservoir C.

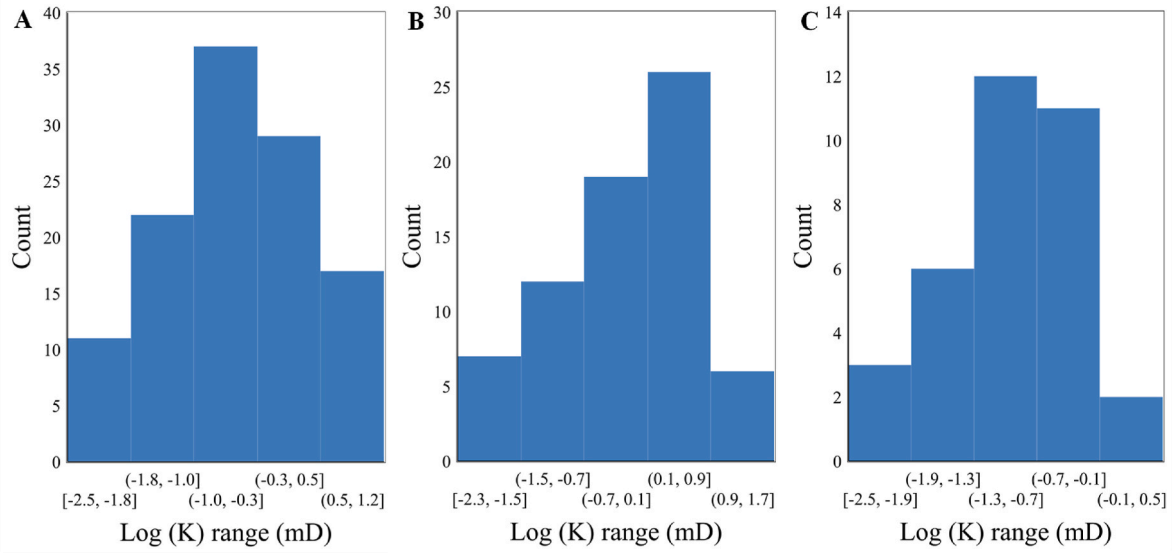

Fig. 3. Log(K) histogram for samples from (A) Reservoir A, (B) Reservoir B, and (C) Reservoir C.

Table 1
Lower RQI boundaries for different rock types and corresponding colors.

GHE* Number	RQI (micrometer), lower limits	Color
10	87.405	
9	29.135	
8	9.712	
7	3.237	
6	1.079	
5	0.360	
4	0.120	
3	0.040	
2	0.013	
1	0.004	

introduced a modified FZI (called FZI* or FZI-star that is identical to RQI).

Primary drainage capillary pressure measurements were also used to study the initial fluid saturation and core quality (Purcell, 1949; Brown, 1951; Skalinski et al., 2014). However, small-scale properties that affect viscous displacements (i.e., dynamic behavior) may not play a key role in capillary-dominated measurements. Moreover, as primary drainage capillary pressure curves are measured on water-wet rocks (i.e., no crude aging), the influence of wettability, which affects both the rate of fluid displacement and residual saturations, is not taken into account (Hamon and Bennes, 2004; Masalmeh and Jing, 2004; Ghedan, 2007; Gomes et al., 2008; Mirzaei-Paiaman et al., 2018, 2019a, 2019b; Faramarzi-Palangar and Mirzaei-Paiaman, 2021).

Some studies have considered certain characteristics of primary drainage capillary pressure curve to determine rock quality, e.g., threshold pressure, irreducible wetting phase saturation, curvature, and inflection point (Thomeer, 1960; Kolodzie, 1980; Swanson, 1981; Ghanbarian et al., 2019; Liu et al., 2020; Abuamarah and Nabawy, 2021). Mirzaei-Paiaman et al. (2018) introduced an index (called PSRTI) by merging Kozeny-Carman equation and Young-Laplace capillary pressure relationship. PSRTI needs porosity, permeability, hydraulic tortuosity, and shape factor as input parameters. Several studies established empirical relationships among a characteristic pore throat size, porosity, and permeability (Kolodzie, 1980; Pittman, 1992; Aguilera, 2002; Jaya et al., 2005; Ngo et al., 2015; Tran et al., 2020; Liu et al., 2020). Among such correlations, the most widely used one is Winland r35 given by Kolodzie (1980).

$$Log(r_{35}) = -0.996 + 0.588\,\mathrm{Log}(k) - 0.864\,Log(\varphi) \tag{3}$$

where r_{35} is the pore size corresponding to 35% mercury saturation on mercury intrusion porosimetry curve.

Rock quality is one of the main factors affecting capillary-driven displacement (Handy, 1960; Cai et al., 2014; Hamidpour et al., 2015, 2018; Abbasi et al., 2017; Harimi et al., 2019). Analyzing spontaneous imbibition experiments may provide information about rock quality (Akin et al., 2000; Roychaudhuri et al., 2013; Hu and Ewing, 2014; Liu et al., 2015; Mirzaei-Paiaman and Saboorian-Jooybari, 2016; Liu, 2017). Imbibition and secondary drainage capillary pressure curves were recently used to study the quality of rocks. If capillary pressure is plotted versus movable hydrocarbon saturation, the relative position of the curve can reveal rock quality (Mirzaei-Paiaman and Ghanbarian, 2021a).

Rock typing may also be performed using relative permeability measurements (Mirzaei-Paiaman et al., 2019b; Yokeley et al., 2021; Mirzaei-Paiaman and Ghanbarian, 2021b). Mirzaei-Paiaman et al. (2019b) introduced true effective mobility (TEM) function through which relative permeability measurements are converted into new curves called TEM.

$$TEM_{\alpha} = \frac{\mathrm{K}k_{r\alpha}}{\varphi\mu_{\alpha}} \tag{4}$$

TEM is a function of saturation and can be calculated for each fluid phase (α) from relative permeability (k_r), permeability, porosity and viscosity (μ). Rocks with similar TEM curves are expected to have identical qualities. Although one can compare fluids displacement rates by analyzing TEM data, in this approach the role of movable fluid saturation has not been taken into account. Furthermore, since TEM is

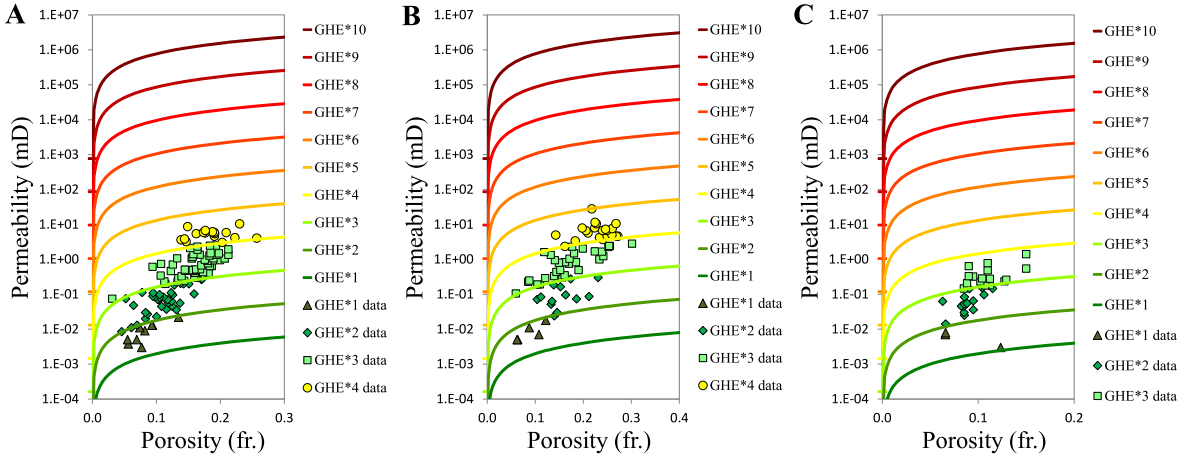

Fig. 4. Distribution of samples on the GHE* template (single-phase rock typing) for (A) Reservoir A, (B) Reservoir B, and (C) Reservoir C. Each line on the template shows the lower boundary of a rock type.

Table 2
Types and properties of the fluids used in the flooding tests.

Reservoir	Brine salinity (gr/L)	Brine density (gr/cc)	Brine viscosity (cp)	Oil type	Oil density (gr/cc)	Oil viscosity (cp)
A	200, 210 or 230	1.15 or 1.17	1.26, 1.40, 1.46, 1.56 or 1.60	Synthetic, kerosene, or dead crude	0.8 or 0.9	1.2, 1.3, 1.4 or 2.5
B	260	1.20	1.64 to 1.88	Synthetic	0.8	1.40 or 2.05
C	200	1.15	0.54 or 1.40	Dead crude or kerosene	0.80 or 0.85	1.30 or 3.82

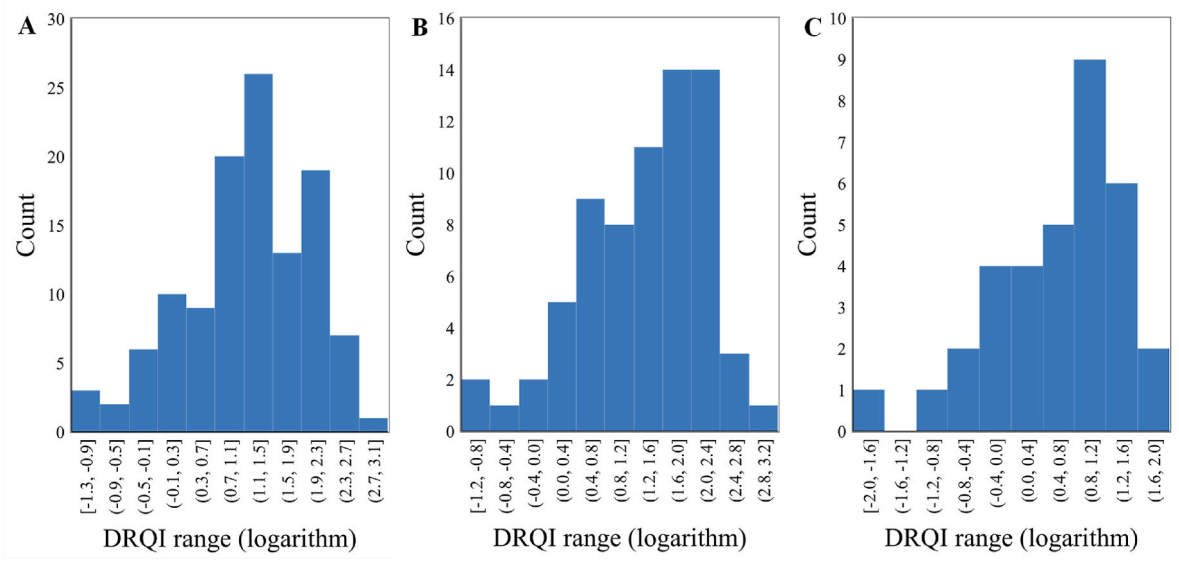

Fig. 5. Histogram of log (DRQI) for the samples from (A) Reservoir A, (B) Reservoir B, and (C) Reservoir C.

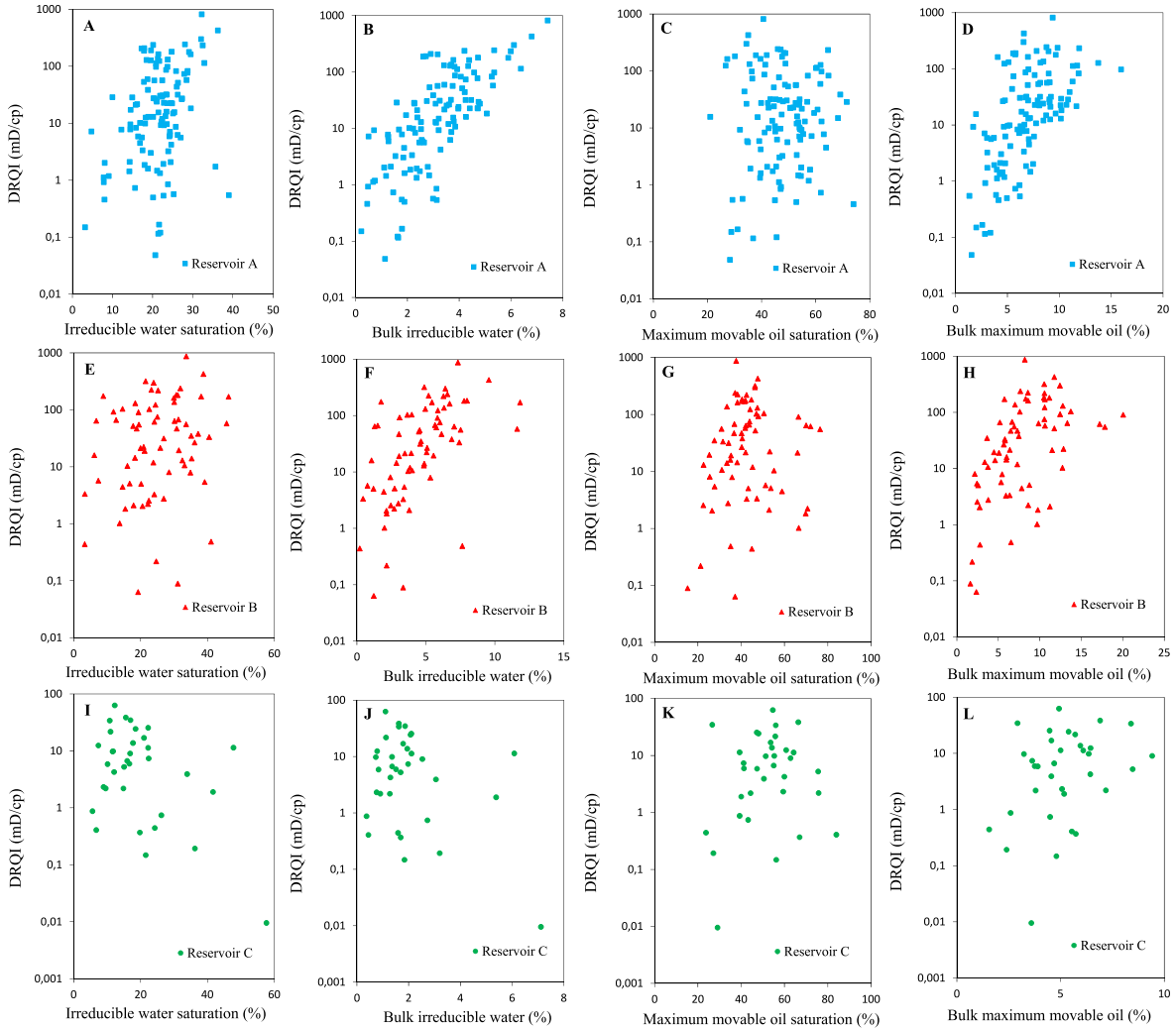

Fig. 6. DRQI versus irreducible water saturation (A, E and I), bulk irreducible water (B, F and J), maximum movable oil saturation (C, G and K), and bulk maximum movable oil (D, H and L) for each of the studied reservoirs.

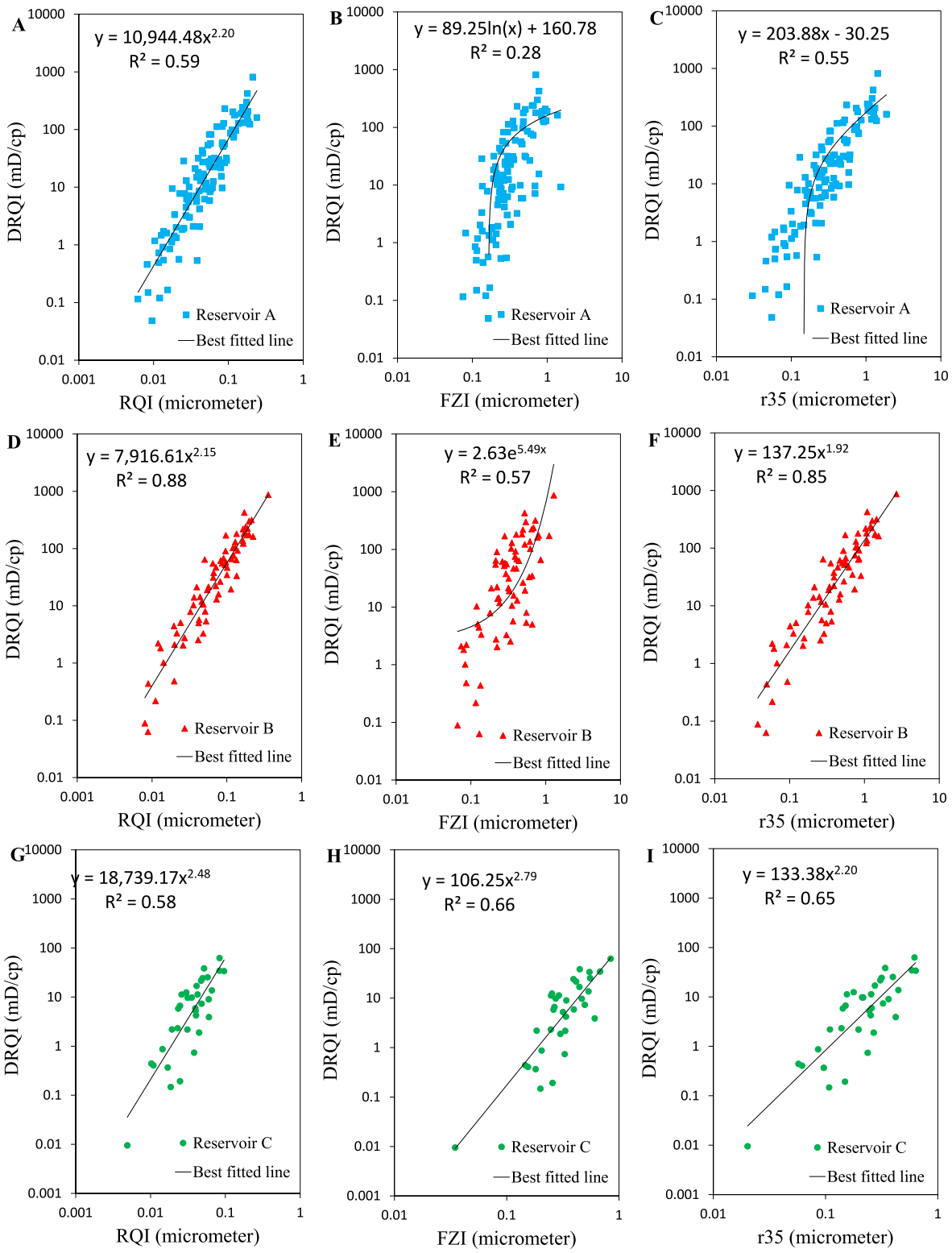

Fig. 7. DRQI versus RQI (A, D and G), FZI (B, E and H), and Winland r35 (C, F and I) for each of the studied reservoirs.

calculated for each fluid phase separately (e.g., CO_2 TEM and water TEM in a CO_2-water displacement), a two-phase system should be practically represented by a pair of curves. Comparing displacement rates of different systems would, therefore, require comparing their corresponding pairs of curves qualitatively. In heterogeneous systems such a comparison may not be conclusive since a rock may have a higher TEM curve for one fluid (e.g., CO_2), while it may show an inferior TEM curve for another one (e.g., water).

The concept of rock quality has been incorporated in reservoir simulation models for well placement optimization by generating so-called quality maps to evaluate productivity/injectivity potentials of grid cells (Babu and Odeh, 1989; Martini et al., 2005; Min et al., 2011; Ding et al., 2014; Pouladi et al., 2020; Oliveira et al., 2021;). Generally, three approaches of numerical simulation, analytical models, and

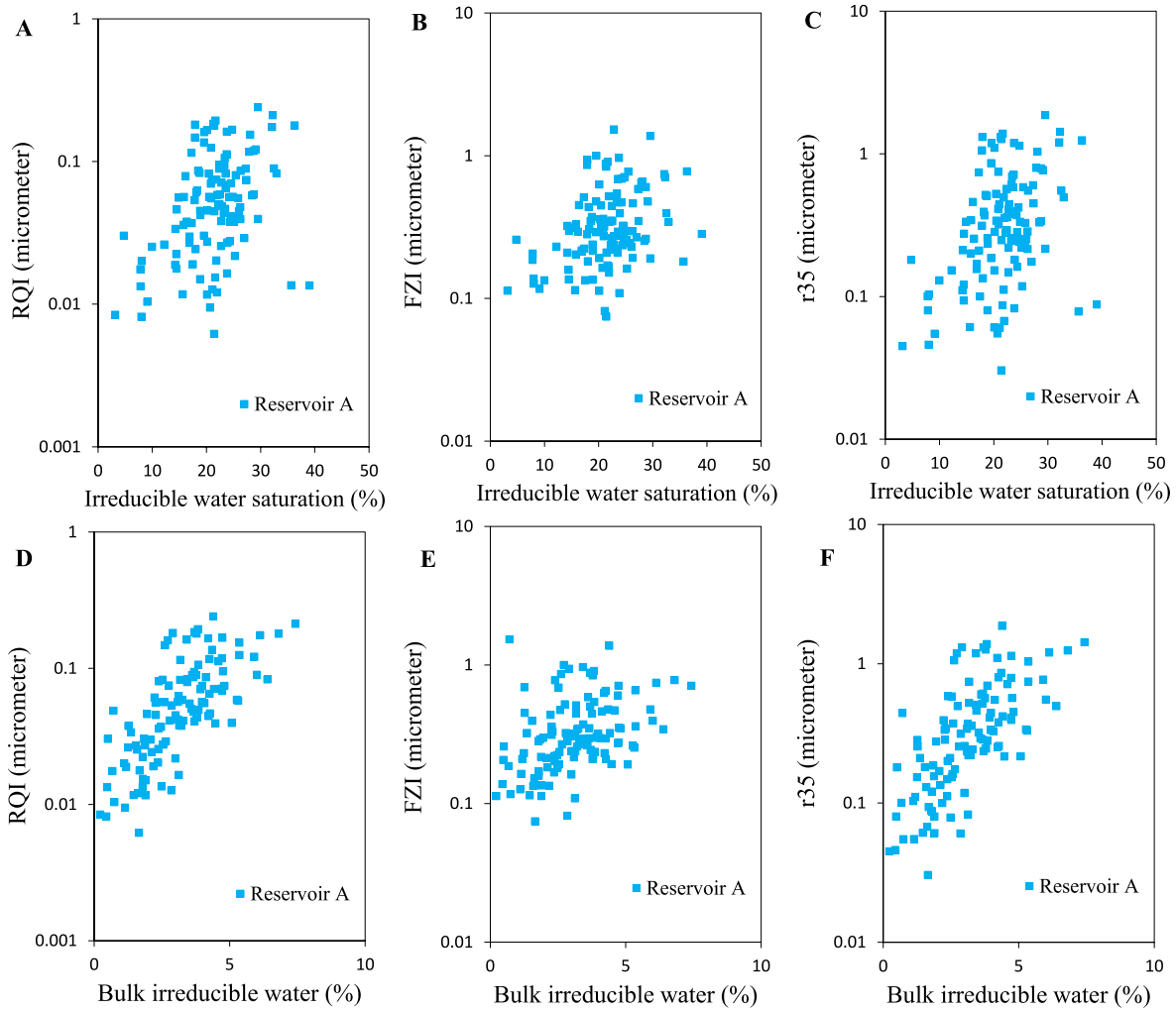

Fig. 8. (A) RQI versus irreducible water saturation, (B) FZI versus irreducible water saturation, (C) Winland r35 versus irreducible water saturation, (D) RQI versus bulk irreducible water, (E) FZI versus bulk irreducible water, and (F) Winland r35 versus bulk irreducible water for Reservoir A.

parametric groups have been used to obtain quality maps. In numerical simulation technique, a reservoir is simulated and quality of different regions is assessed by evaluating simulation outputs (Nakajima and Schiozer, 2003; da Cruz et al., 2004; Ravalec, 2012). The main limitation of defining quality map using the simulation outputs is the associated computational cost. Furthermore, in such an approach usually only cumulative produced/injected volumes are considered as quality criteria. Quality maps derived from analytical models are mainly focused on flow rates in pressure depletion scenarios (Nakajima and Schiozer, 2003). Some studies have combined basic properties, such as permeability, porosity, initial fluids saturation, thickness, and pressure, to form parametric groups for describing reservoir quality (Cullick et al., 2005; Liu and Jalali, 2006; Narayanasamy et al., 2006; Maschio et al., 2008). These groups are not unique, so numerous forms of them can be defined arbitrarily, and that the parameters focus on initial saturation and deliverability in single-phase flows.

Quality of a reservoir is typically defined by its hydrocarbon storage capacity and deliverability (Gluyas and Swarbrick, 2004; Blackbourn, 2012; Worden et al., 2018). However, hydrocarbon storage capacity does not necessarily represent the recoverable hydrocarbon capacity. To the best of the authors' knowledge, there exists no index that takes into account the effect of both (i) displacement rate and (ii) displaceable fluid saturation in multiphase applications. Therefore, in this paper, reservoir quality is defined by hydrocarbon recoverable (or displaceable/movable) capacity and deliverability (or displacement rate). Consequently, a high-quality reservoir rock is expected to be associated with a high rate of hydrocarbon recovery and high recoverable hydrocarbon saturation. By accounting for these two factors, a new approach called dynamic reservoir quality index (DRQI) is proposed with applications to multiphase flow.

2. Model development

Let us consider a horizontal system where oil is immiscibly displaced by another fluid (e.g., water). Oil fractional flow, f_o, can be expressed as oil flow rate (q_o) normalized by total water and oil flow rates ($q_o + q_w$) (Dullien, 1992; Blunt, 2017) as follows.

$$f_o = \frac{q_o}{q_o + q_w} = \frac{1}{1 + \frac{k_{rw}}{k_{ro}}\frac{\mu_o}{\mu_w}} \tag{5}$$

where the subscripts w and o refer to water and oil, respectively. For the displacement of oil by gas, one may simply substitute the subscript w by g.

Following Eq. (4), the maximum true effective mobility of oil (TEM_o^{max}) occurs at the irreducible water saturation S_{wir} (where water is immobile) and can be written as

$$TEM_o^{max} = \frac{Kk_{ro}^{max}}{\varphi\mu_o} \tag{6}$$

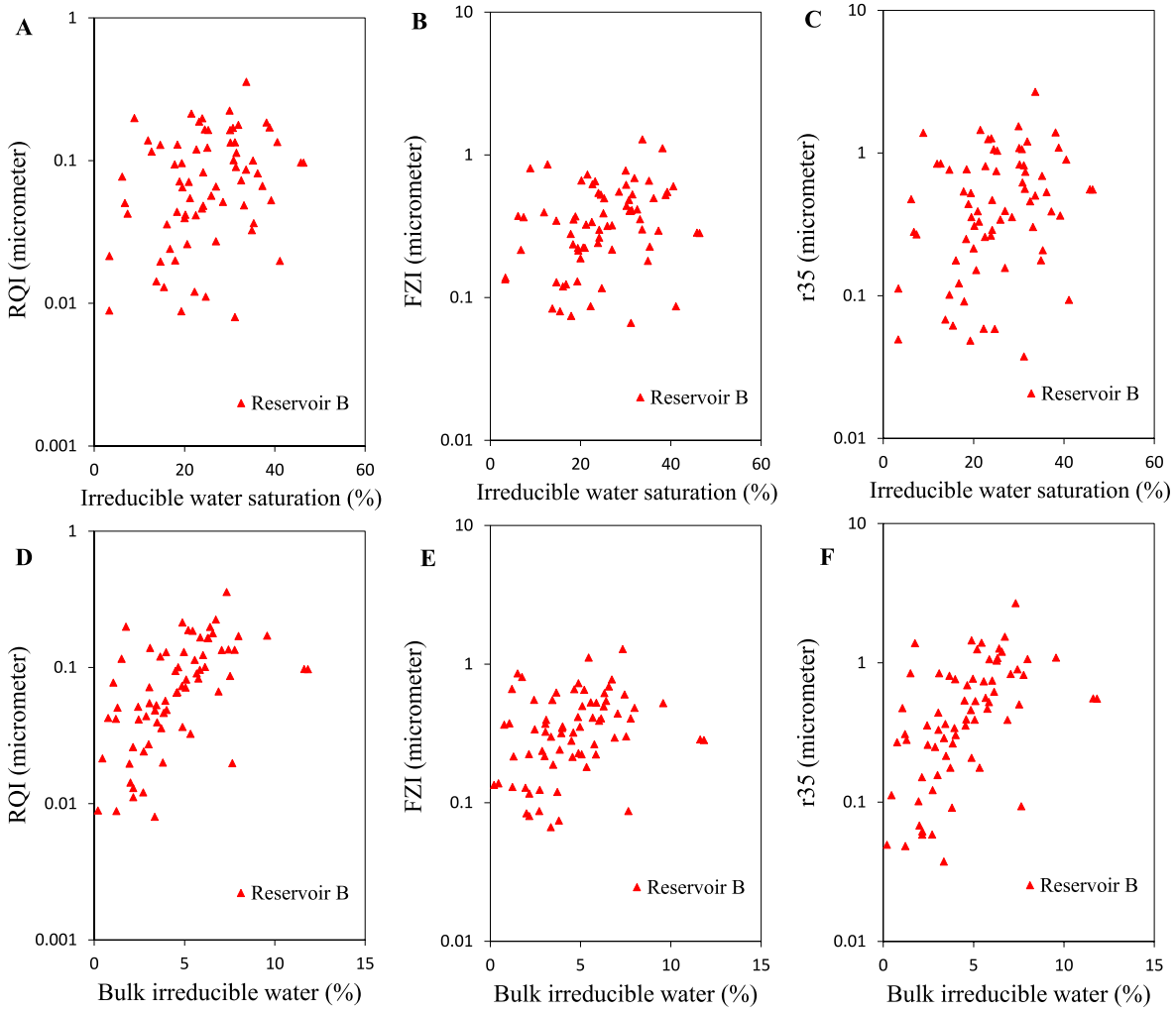

Fig. 9. (A) RQI versus irreducible water saturation, (B) FZI versus irreducible water saturation, (C) Winland r35 versus irreducible water saturation, (D) RQI versus bulk irreducible water, (E) FZI versus bulk irreducible water, and (F) Winland r35 versus bulk irreducible water for Reservoir B.

k_{ro}^{max} is the maximum oil relative permeability (i.e., k_{ro} at S_{wir}). In our analysis, relative permeability is defined as the effective permeability divided by the absolute permeability.

As f_o is dimensionless, multiplying it by TEM_o^{max} leads to a reasonable basis for comparing oil-by-water displacement rates of different systems. Thus, aiming at developing a robust function to estimate the rate at which oil is displaced by another fluid, the modified oil TEM (TEM_o^*) can then be written as:

$$TEM_o^* = TEM_o^{max} f_o = \frac{Kk_{ro}^{max}}{\varphi\mu_o}\left(\frac{1}{1+\frac{k_{rw}}{k_{ro}}\frac{\mu_o}{\mu_w}}\right) \tag{7}$$

The important feature of the modified oil TEM is that it combines both water and oil relative permeability curves into a single curve, in contrast to the usual TEM which is individually determined for each phase. Comparing modified oil TEMs of different rocks provides the basis to assess their dynamic behaviors. At two endpoints irreducible water saturation and residual oil saturation, TEM_o^* reduces to TEM_o^{max} and zero, respectively.

To appropriately account for both oil displacement rate and movable oil saturation, the dynamic reservoir quality index (DRQI) is proposed by integrating the curve of TEM_o^* from the initial water saturation (S_{wi}) to the final water saturation ($1 - S_{or}$) to have

$$DRQI = \int_{S_{wi}}^{1-S_{or}} TEM_o^*\, dS_w = \frac{Kk_{ro}^{max}}{\varphi\mu_o}\int_{S_{wi}}^{1-S_{or}} \frac{1}{1+\frac{k_{rw}}{k_{ro}}\frac{\mu_o}{\mu_w}}\, dS_w \tag{8}$$

In Eq. (8), DRQI is expressed in mD/cp, and S_{or} is the residual oil saturation. We note that S_{wir} is a special case of S_{wi} (i.e., $S_{wir} \le S_{wi}$). Fig. 1 shows DRQI defined as the area under the modified oil TEM curve. For a system or grid cell in an oil zone with no previous experience of saturation change due to waterflooding, one would have $S_{wi} = S_{wir}$. For such a system with previous experience of saturation change or a system within a water-oil transition zone one would have $S_{wi} > S_{wir}$.

For a given rock (or grid cell in simulation model), DRQI could be time-dependent because S_{wi} may vary with time. As DRQI increases, the dynamic rock quality increases as well. It is noteworthy to mention that in this study the modified TEM of oil is considered as the indicator of dynamic reservoir quality. This is because displacement rate and recoverable saturation of oil is of interest in water-oil displacement processes. However, the proposed approach can be extended to three phases and other applications, e.g., CO_2 injection into aquifers or waterflooding of gas reservoirs, by determining the modified TEM for a desired fluid.

By replacing K/φ from Eq. (1) in Eq. (8), it will be

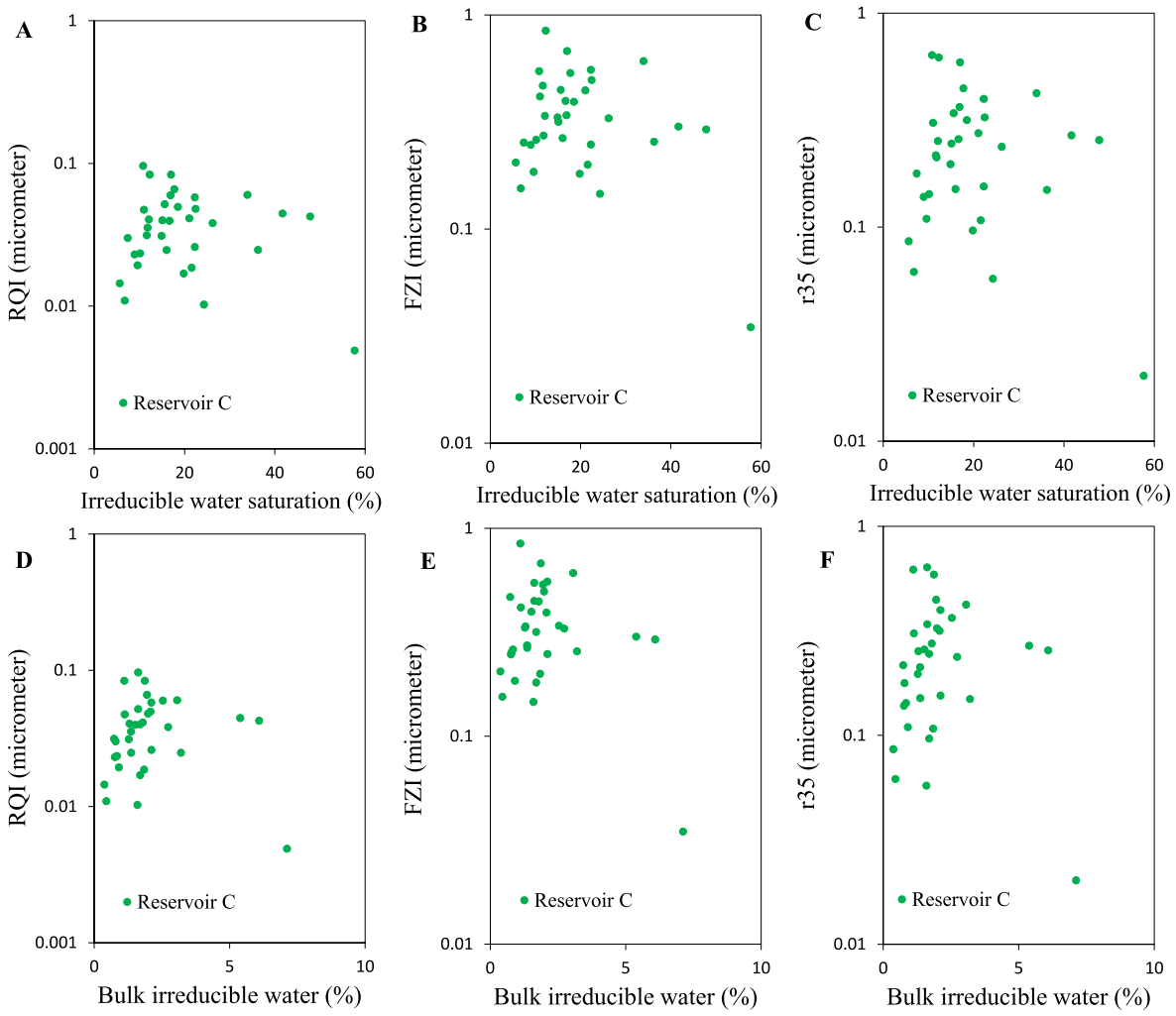

Fig. 10. (A) RQI versus irreducible water saturation, (B) FZI versus irreducible water saturation, (C) Winland r35 versus irreducible water saturation, (D) RQI versus bulk irreducible water, (E) FZI versus bulk irreducible water, and (F) Winland r35 versus bulk irreducible water for Reservoir C.

$$DRQI = 1014\, RQI^2 \frac{k_{ro}^{max}}{\mu_o} \int_{S_{wi}}^{1-S_{or}} \frac{1}{1+\frac{k_{rw}}{k_{ro}}\frac{\mu_o}{\mu_w}} dS_w \quad (9)$$

Eq. (9) indicates that RQI is a special case of DRQI. Eq. (9) clearly shows that in addition to RQI, there is the necessity of bringing two-phase characteristics of system (i.e., relative permeabilities, fluids viscosities, and initial and final saturations) into the quality analysis.

3. Materials and experiments

220 limestone and dolomite plug samples (1.5 in diameter and 2 in length) from three Iranian reservoirs, named A, B and C, were used. The number of samples in reservoirs A, B, and C are respectively 116, 70, and 34. The samples were first cleaned and dried according to API recommended practice RP40 Standard (API, 1998) followed by measuring helium porosity and permeability. The salient properties of the samples are summarized in Tables A-1, A-2, and A-3 for reservoirs A, B, and C, respectively (see Appendix 1). Porosity and permeability ranged from 3 to 26% and 0.003 to 10.458 mD for Reservoir A, 6 to 30% and 0.01 to 28.14 mD for Reservoir B, and 6 to 15% and 0.003 to 1.410 mD for reservoir C. The measured data confirm a wide spectrum of petrophysical properties for the three studied reservoirs. The histograms of porosity and permeability for the three reservoirs are shown in Figs. 2 and 3, respectively.

The porosity and permeability data were used to identify single-phase rock types using the GHE* method. The global hydraulic element (GHE) technique proposed by Corbett and Potter (2004) is based on dividing a wide range of FZI values into 10 clusters or GHE classes. In such a graphical template, GHE1 and GHE10 are placed at the base and top of the porosity-permeability plot, respectively. Core plugs and petrophysical data can be plotted in clusters between the pre-determined GHE lines. GHE mapping approach allows rock typing and a comparison between reservoirs, wells, fields, and core and simulation data on the basis of FZI values. Mirzaei-Paiaman et al. (2020) proposed the GHE* technique based on RQI or FZI* values. In their approach, a wide range of RQI values are classified into 10 reference single-phase rock types or GHE*s. The difference between the GHE and GHE* techniques is that the former is based on FZI whereas the later on the basis of RQI values. Table 1 summarizes the lower RQI limits and color of each pre-defined GHE* class. To set these boundaries, the broadest possible range of RQI was considered. GHE*10 is open-ended and does not have an upper limit. If RQI values smaller than 0.004 are encountered, the lower limit of the first GHE* can be disregarded, too.

The rock type or GHE* class number corresponding to each sample is included in Tables A-1 to A-3. The distribution of samples on the GHE* template is shown in Fig. 4 for the three reservoirs. Each line on the template represents the lower boundary of a pre-built reference rock type, see Table 1. As can be seen, the samples are distributed in rock types 1, 2, 3 and 4 for Reservoirs A and B, and rock types 1, 2 and 3 for Reservoir C.

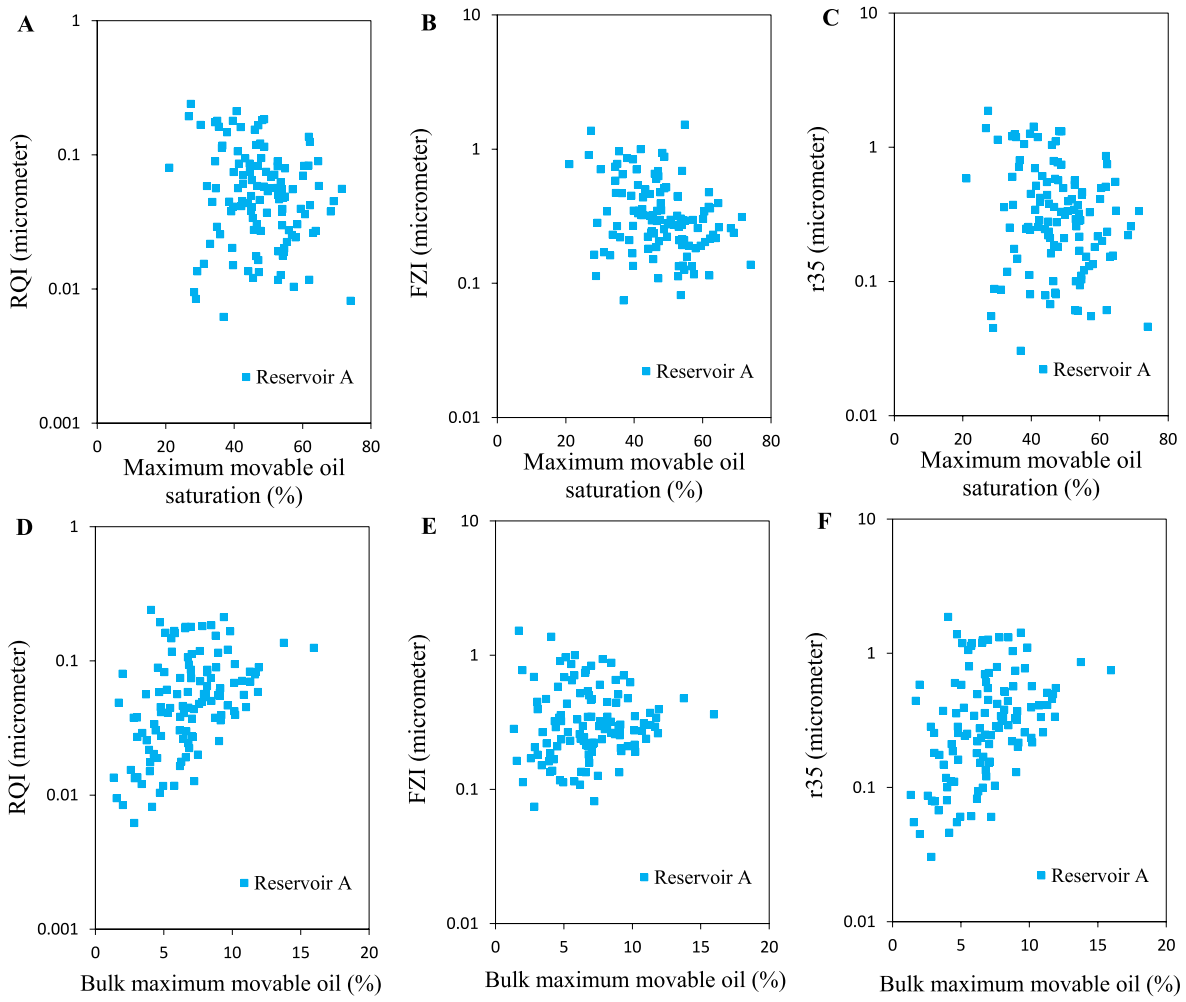

Fig. 11. (A) RQI versus maximum movable oil saturation, (B) FZI versus maximum movable oil saturation, (C) Winland r35 versus maximum movable oil saturation, (D) RQI versus bulk maximum movable oil, (E) FZI versus bulk maximum movable oil, and (F) Winland r35 versus bulk maximum movable oil for Reservoir A.

The cleaned and dried samples were saturated with synthetic brine (NaCl solution) and soaked for at least 10 days to achieve ionic equilibrium between the solution and minerals. Consequently, using a centrifuge set-up, stock tank crude displaced the brine until reaching irreducible water saturation. Aiming at restoring the native reservoir wetting state, some samples were submerged in crude oil in aging cells at the reservoir temperature of 70 °C for 15 days. In order to establish a uniform wetting condition, crude was flushed through the plugs twice during the aging test. Then, the crude was replaced by an oleic fluid. For some of the samples no aging was performed to keep samples water-wet. As a result, our database contains both water-wet and non-water-wet samples. Afterwards, the unsteady-state primary imbibition water-oil relative permeability experiments were performed using brine and oleic fluid at 25 °C. The experiments were continued until reaching residual oil saturation. Produced fluids, time and pressure data were recorded and used to calculate relative permeability data using Jones and Roszella (1978) method. Details about unsteady-state relative permeability tests can be found elsewhere (e.g., McPhee et al., 2015). Types and properties of the fluids (i.e., salinity, density and viscosity) that were used in the flooding tests are summarized in Table 2. Further details regarding the aging condition, irreducible water saturation and residual oil saturation for the conducted relative permeability tests are summarized in Tables A-1, A-2 and A-3.

4. Results and discussion

4.1. The DRQI histograms

For each sample, TEM_o^* was determined from water and oil relative permeability curves as well as other rock and fluid properties via Eq. (7). Next, DRQI for each sample was determined from the area under TEM_o^* curve using Eq. (8). The studied rock samples were from oil zones with no previous saturation change due to the absence of water-flooding or aquifer rise. Accordingly, $S_{wi} = S_{wir}$ was assumed to calculate DRQI. Tables A-1, A-2 and A-3 list DRQI values as well as other indices i.e., RQI, FZI, and Winland r35 for the samples. The samples represent a wide range of dynamic qualities from 0.05 to 816.59 mD/cp for Reservoir A, 0.06 to 867.90 mD/cp for Reservoir B, and 0.01 to 62.68 mD/cp for Reservoir C. Fig. 5 displays the histogram for the log (DRQI).

4.2. Comparing DRQI with other reservoir quality indices

In this section, DRQI is compared with other commonly-used reservoir quality indicators i.e., irreducible water saturation (S_{wir}), maximum movable oil saturation ($1 - S_{wir} - S_{or}$), RQI, FZI, and Winland r35. Recall that the bulk irreducible water is $S_{wir}\varphi$, and the bulk maximum movable oil is $(1 - S_{wir} - S_{or})\varphi$. A routine practice in industry (Jadhunandan and Morrow, 1995; Skauge and Ottesen, 2002; Zhao et al., 2010; Armstrong et al., 2021) is comparing petrophysical properties (e.g., wettability index) with residual oil saturation S_{or} and recovery factor ($(1 - S_{wir} -$

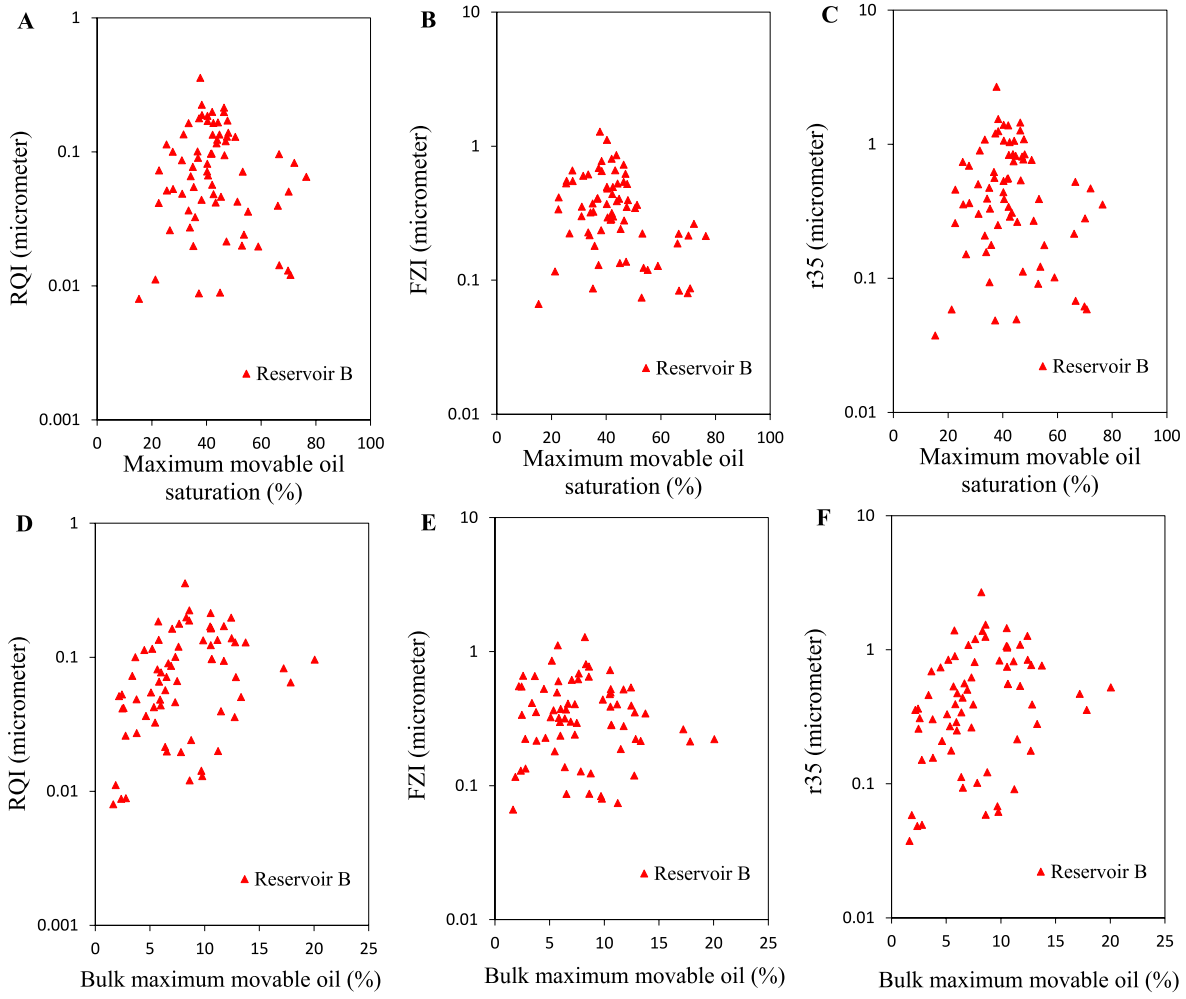

Fig. 12. (A) RQI versus maximum movable oil saturation, (B) FZI versus maximum movable oil saturation, (C) Winland r35 versus maximum movable oil saturation, (D) RQI versus bulk maximum movable oil, (E) FZI versus bulk maximum movable oil, and (F) Winland r35 versus bulk maximum movable oil for Reservoir B.

$S_{or})/(1 - S_{wir})$). However, in this study neither DRQI nor other rock quality indicators, i.e., RQI, FZI and Winland r35, are compared to these variants of saturation. This is because such a comparison could be misleading, particularly under circumstances where samples have nonidentical S_{wir} values. In fact, S_{or} is the final state of saturation, and comparing final states of rocks, regardless of their initial states (i.e., S_{wir}), is not supported. Moreover, recovery factor by definition is the amount of the produced oil normalized by the initial oil in place. As systems with nonidentical values of S_{wir} have dissimilar amounts of initial oil in place, comparing their recovery factors is difficult and should be avoided. Mirzaei-Paiaman and Ghanbarian (2021a) showed that in primary drainage process (where oil displaces water from an initially fully water-saturated rock), the appropriate parameter to explore possible correlations with other factors would be S_{wir}. Similarly, in subsequent imbibition process (where water displaces oil from the system which is initially at irreducible water saturation) the proper parameter is $1 - S_{wir} - S_{or}$.

In Fig. 6, DRQI is plotted against irreducible water saturation and bulk irreducible water, as well as maximum movable hydrocarbon saturation and bulk maximum movable hydrocarbon for each of the three reservoirs, separately. As can be observed, the data are highly scattered and no clear trends can be observed between DRQI and these parameters. This confirms that irreducible water saturation and maximum movable hydrocarbon saturation, and also their bulk forms, might lead to inaccurate characterizations of dynamic reservoir quality and, therefore, should not be used.

To investigate the relationship between DRQI and single-phase rock quality indicators, cross-plots showing DRQI versus RQI, FZI, and Winland r35 for each reservoir are presented in Fig. 7. In each plot, the best fitted line to the data and the corresponding coefficient of determination (R^2) are also displayed. Generally speaking, as RQI, FZI and r35 values increase, DRQI increases as well. In the case of Reservoir A, DRQI showed better correlations with RQI ($R^2 = 0.59$) and r35 ($R^2 = 0.55$) than FZI ($R^2 = 0.28$). Likewise, for Reservoir B, DRQI showed better correlations with RQI ($R^2 = 0.88$) and r35 ($R^2 = 0.85$) than FZI ($R^2 = 0.57$). Regarding Reservoir C, DRQI showed almost similar correlations with RQI ($R^2 = 0.58$), FZI ($R^2 = 0.66$) and r35 ($R^2 = 0.65$). It was noted that at a given value of RQI, FZI or r35, DRQI varies by more than one order of magnitude. One may also notice that while most values of DRQI span four orders of magnitude in variation, RQI, FZI, and r35 span only around two orders of magnitude. The results confirm that generally single-phase indicators might sometimes lead to inaccurate characterizations of dynamic reservoir quality. Thus, if relative permeabilities are not available to determine TEM_0^* and consequently DRQI, one should use RQI, r35, or FZI with caution.

4.3. *Comparing routine reservoir quality indices with irreducible/residual content*

The large number of samples and the variety of data allow us to investigate the relationships between each routine rock typing index and S_{wir}, $S_{wir}\varphi$, $1 - S_{wir} - S_{or}$, and $(1 - S_{wir} - S_{or})\varphi$. Plots of RQI, FZI and

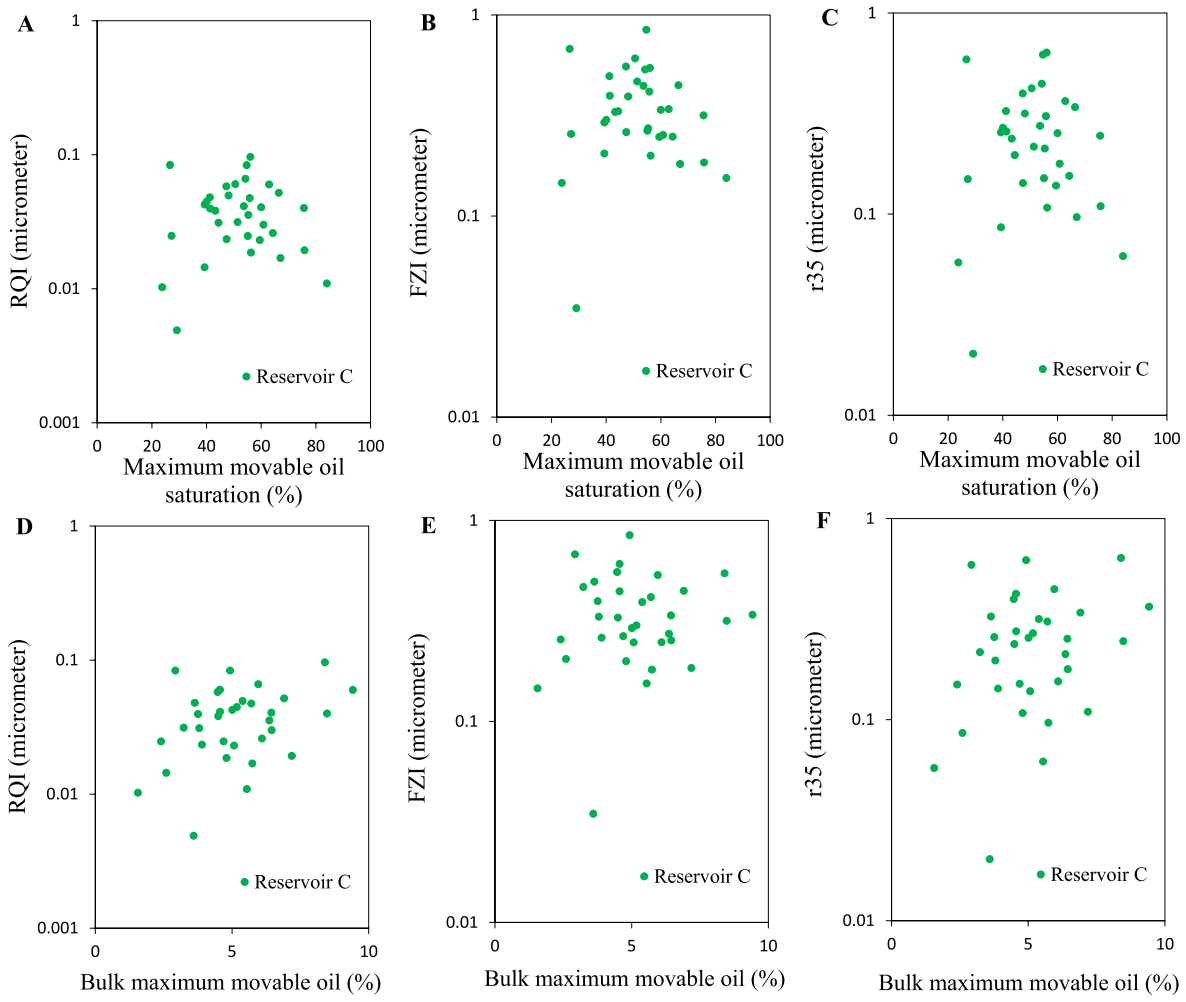

Fig. 13. (A) RQI versus maximum movable oil saturation, (B) FZI versus maximum movable oil saturation, (C) Winland r35 versus maximum movable oil saturation, (D) RQI versus bulk maximum movable oil, (E) FZI versus bulk maximum movable oil, and (F) Winland r35 versus bulk maximum movable oil for Reservoir C.

Winland r35 versus irreducible water saturation and its bulk variant are shown in Figs. 8–10 for Reservoirs A, B and C, respectively. Furthermore, plots of RQI, FZI and Winland r35 versus maximum recoverable oil saturation and its bulk variant are shown in Figs. 11–13 for Reservoirs A, B and C, respectively. Since the data are highly scattered, no apparent correlations exist between the routine rock quality indices and saturation and bulk parameters.

5. Conclusion

In this study, the problem of dynamic reservoir quality was addressed. A high dynamic quality reservoir rock was defined as a system associated with a high rate of oil recovery and high recoverable oil saturation. The modified oil TEM was proposed that estimates the rate at which oil is displaced by another fluid. To appropriately account for both oil displacement rate and movable oil saturation, the area under modified oil TEM curve was used to define a new index named DRQI.

A large dataset including water-oil relative permeability experiments on 220 limestone and dolomite samples from three reservoirs was used to investigate the potential relationships between DRQI and other reservoir quality parameters, such as irreducible water saturation, bulk irreducible water, maximum movable oil saturation, bulk movable oil saturation, RQI, FZI, and Winland r35. Results showed that irreducible water saturation and maximum movable oil saturation as well as their bulk variants may not be appropriate to characterize multiphase reservoir quality. Similarly, it was found that the frequently-used single-phase rock quality indicators i.e., RQI, FZI and Winland r35 were not very accurate in the characterization of dynamic reservoir quality. RQI, FZI and Winland r35 were plotted versus irreducible water saturation, bulk irreducible water, maximum movable oil saturation, bulk movable oil saturation and no apparent correlations were found.

DRQI tries to capture the dynamic quality of reservoir rocks with applications to multiphase flow where oil is displaced by another fluid (e.g., aquifer encroachment, gas-cap expansion, and secondary and tertiary recovery processes). Comparing DRQI values from different rocks provides the basis for assessing their dynamic qualities. This has applications to the preparation of quality maps in the context of reservoir simulation as well as rock typing studies.

Author statement

Abouzar Mirzaei-Paiaman: Conceptualization, Methodology, Validation, Formal analysis, Investigation, Writing – original draft, Writing – review & editing. **Behzad Ghanbarian**: Conceptualization, Methodology, Validation, Formal analysis, Investigation, Writing – original draft, Writing – review & editing.

Declaration of competing interest

The authors declare that they have no known competing financial interests or personal relationships that could have appeared to influence the work reported in this paper.

Data availability

The data is available in this link for the peer-review process https://osf.io/j6bp7/?view_only=900ff4c6281c4952a9c4e2b3e4aba8d4 and will become public after acceptance

Acknowledgement

Behzad Ghanbarian is grateful to Kansas State University for the faculty startup fund.

Appendix 1

Table A-1
Properties of the rocks and flow displacement experiments (Reservoir A).

Test ID	φ (fr.)	K (mD)	Crude aging	S_{wi} (%)	S_{or} (%)	DRQI (mD/cp)	RQI (μm)	FZI (μm)	r35 (μm)	GHE* no.
1	0.08	0.003	Yes	21.43	41.67	0.115	0.006	0.074	0.030	1
2	0.06	0.004	Yes	8.00	17.99	0.457	0.008	0.138	0.046	1
3	0.07	0.005	Yes	3.18	67.98	0.149	0.008	0.113	0.045	1
4	0.05	0.005	Yes	20.69	50.99	0.048	0.009	0.164	0.055	1
5	0.08	0.009	Yes	9.09	33.47	1.179	0.010	0.117	0.055	1
6	0.09	0.013	No	20.11	27.06	0.496	0.012	0.113	0.061	1
7	0.09	0.013	Yes	15.63	22.41	0.730	0.012	0.114	0.061	1
8	0.07	0.011	Yes	21.92	32.52	0.120	0.012	0.151	0.068	1
9	0.13	0.022	No	21.13	25.27	1.466	0.013	0.082	0.061	1
10	0.06	0.011	Yes	7.84	44.96	0.922	0.013	0.206	0.080	2
11	0.05	0.009	No	39.02	31.74	0.545	0.014	0.283	0.088	2
12	0.07	0.013	No	35.66	20.19	1.728	0.014	0.181	0.079	2
13	0.10	0.023	No	18.85	41.49	1.598	0.015	0.135	0.080	2
14	0.08	0.020	Yes	21.62	47.24	0.166	0.015	0.170	0.087	2
15	0.13	0.036	Yes	23.81	29.13	0.846	0.016	0.109	0.083	2
16	0.09	0.027	Yes	7.80	45.74	1.117	0.018	0.186	0.100	2
17	0.12	0.037	No	14.47	31.32	9.510	0.018	0.136	0.094	2
18	0.08	0.030	No	14.22	31.20	1.431	0.019	0.209	0.111	2
19	0.12	0.046	Yes	17.50	29.51	3.338	0.019	0.134	0.100	2
20	0.14	0.056	No	8.06	37.27	2.016	0.020	0.127	0.103	2
21	0.11	0.045	No	21.85	38.69	1.325	0.020	0.168	0.112	2
22	0.12	0.057	No	25.24	41.77	0.566	0.022	0.162	0.118	2
23	0.12	0.063	No	14.45	30.15	7.786	0.022	0.159	0.121	2
24	0.12	0.070	Yes	18.02	24.02	1.847	0.024	0.182	0.135	2
25	0.16	0.103	No	9.98	33.12	28.647	0.025	0.134	0.130	2
26	0.10	0.069	No	22.71	41.40	1.930	0.026	0.220	0.148	2
27	0.10	0.071	No	12.21	24.74	7.741	0.026	0.231	0.153	2
28	0.06	0.048	Yes	23.91	28.37	3.219	0.027	0.395	0.181	2
29	0.11	0.083	No	16.87	19.29	4.497	0.027	0.217	0.156	2
30	0.13	0.096	No	20.13	23.85	12.964	0.027	0.191	0.153	2
31	0.10	0.081	No	24.35	29.91	6.232	0.028	0.235	0.162	2
32	0.10	0.084	No	27.00	38.02	5.602	0.029	0.268	0.175	2
33	0.12	0.111	No	16.88	29.07	10.135	0.030	0.213	0.170	2
34	0.09	0.088	No	19.54	33.85	3.026	0.030	0.291	0.186	2
35	0.11	0.098	Yes	4.76	36.74	7.170	0.030	0.258	0.180	2
36	0.09	0.110	Yes	14.29	40.27	2.100	0.034	0.322	0.211	2
37	0.15	0.199	No	15.78	23.52	20.988	0.036	0.203	0.200	2
38	0.14	0.199	Yes	17.31	33.13	5.610	0.037	0.223	0.210	2
39	0.05	0.075	No	24.31	21.70	7.087	0.038	0.690	0.284	2
40	0.13	0.185	No	25.11	6.63	14.858	0.038	0.257	0.221	2
41	0.08	0.113	No	16.37	44.46	5.866	0.038	0.450	0.255	2
42	0.14	0.205	No	22.73	32.31	0.535	0.038	0.239	0.220	2
43	0.17	0.269	No	26.26	19.65	31.726	0.039	0.193	0.215	2
44	0.17	0.274	No	29.54	11.02	18.249	0.040	0.191	0.216	2
45	0.14	0.243	No	25.78	29.13	8.645	0.041	0.244	0.235	3
46	0.13	0.229	Yes	24.66	35.67	4.193	0.041	0.268	0.242	3
47	0.11	0.198	Yes	24.50	33.40	2.072	0.041	0.323	0.255	3
48	0.16	0.294	Yes	18.89	18.93	12.960	0.042	0.216	0.235	3
49	0.16	0.316	No	23.21	32.80	13.318	0.044	0.223	0.245	3
50	0.16	0.327	No	26.03	40.29	43.713	0.045	0.231	0.252	3
51	0.18	0.358	No	21.45	40.00	15.496	0.045	0.210	0.248	3
52	0.16	0.330	No	18.85	12.04	38.520	0.045	0.239	0.257	3
53	0.11	0.234	No	20.20	37.44	27.434	0.045	0.358	0.284	3
54	0.13	0.290	No	14.52	38.03	17.141	0.046	0.297	0.276	3
55	0.18	0.400	Yes	23.49	23.36	15.940	0.047	0.210	0.257	3
56	0.14	0.324	No	26.24	19.41	6.224	0.048	0.296	0.286	3
57	0.03	0.075	No	22.81	22.39	9.253	0.049	1.527	0.443	3
58	0.17	0.429	Yes	22.22	32.82	10.715	0.049	0.236	0.279	3
59	0.16	0.410	Yes	22.41	24.62	11.931	0.050	0.264	0.291	3
60	0.16	0.466	No	17.85	32.32	53.285	0.054	0.281	0.314	3
61	0.17	0.519	No	20.92	25.15	25.328	0.055	0.272	0.320	3
62	0.16	0.490	No	25.85	17.05	82.413	0.055	0.297	0.328	3

(continued on next page)

Table A-1 (*continued*)

Test ID	φ (fr.)	K (mD)	Crude aging	S_{wi} (%)	S_{or} (%)	DRQI (mD/cp)	RQI (μm)	FZI (μm)	r35 (μm)	GHE* no.
63	0.15	0.481	Yes	14.93	13.59	28.384	0.056	0.313	0.335	3
64	0.11	0.343	No	24.20	41.15	5.884	0.056	0.472	0.372	3
65	0.15	0.469	No	15.85	43.02	8.326	0.056	0.332	0.343	3
66	0.16	0.518	No	24.85	24.56	22.314	0.057	0.298	0.334	3
67	0.15	0.491	No	20.50	26.92	27.336	0.057	0.319	0.341	3
68	0.19	0.636	No	28.46	22.85	57.293	0.058	0.253	0.330	3
69	0.15	0.504	No	22.05	45.92	9.280	0.058	0.343	0.357	3
70	0.14	0.505	No	22.50	30.83	30.880	0.059	0.348	0.359	3
71	0.18	0.642	No	28.72	6.52	82.587	0.059	0.262	0.337	3
72	0.12	0.463	Yes	18.15	39.29	9.886	0.061	0.437	0.393	3
73	0.17	0.676	Yes	18.28	28.15	12.563	0.063	0.304	0.370	3
74	0.18	0.771	No	23.54	31.30	31.758	0.065	0.294	0.380	3
75	0.20	0.953	Yes	23.67	25.54	22.502	0.069	0.275	0.395	3
76	0.19	0.938	No	20.83	19.05	112.010	0.070	0.302	0.411	3
77	0.18	0.907	No	24.57	32.81	22.620	0.071	0.322	0.420	3
78	0.21	1.062	Yes	22.80	25.43	22.752	0.071	0.273	0.408	3
79	0.18	0.984	No	27.37	32.78	27.308	0.074	0.349	0.449	3
80	0.19	1.066	No	21.03	34.37	23.968	0.075	0.319	0.442	3
81	0.13	0.712	No	21.88	28.78	30.324	0.075	0.520	0.496	3
82	0.21	1.353	Yes	16.15	28.98	21.592	0.079	0.294	0.460	3
83	0.09	0.614	No	25.43	53.53	15.627	0.080	0.775	0.585	3
84	0.16	1.063	No	20.44	26.87	56.343	0.082	0.448	0.524	3
85	0.11	0.740	Yes	23.55	29.48	9.681	0.082	0.687	0.582	3
86	0.19	1.348	No	32.91	6.64	113.952	0.083	0.344	0.496	3
87	0.18	1.287	Yes	18.75	19.52	59.277	0.083	0.372	0.508	3
88	0.16	1.173	No	26.32	29.15	51.288	0.086	0.463	0.550	3
89	0.20	1.483	No	18.49	40.12	128.504	0.086	0.349	0.516	3
90	0.13	1.070	Yes	27.27	38.27	26.450	0.089	0.584	0.602	3
91	0.17	1.356	No	22.41	24.88	56.502	0.089	0.444	0.565	3
92	0.18	1.503	No	32.48	2.94	232.150	0.090	0.395	0.552	3
93	0.16	1.415	Yes	23.33	33.41	31.948	0.094	0.501	0.610	3
94	0.21	1.935	No	22.36	29.74	29.322	0.095	0.351	0.567	3
95	0.16	1.880	Yes	23.37	35.56	86.267	0.106	0.540	0.696	3
96	0.19	2.485	No	23.72	39.88	97.758	0.113	0.470	0.713	3
97	0.18	2.468	No	17.26	33.91	204.656	0.115	0.511	0.742	3
98	0.15	2.127	Yes	27.87	35.56	73.452	0.117	0.650	0.798	3
99	0.16	2.334	No	28.72	24.81	77.192	0.118	0.603	0.792	3
100	0.20	3.040	No	29.07	23.29	177.701	0.122	0.477	0.770	4
101	0.26	4.080	Yes	20.85	17.00	97.583	0.125	0.362	0.747	4
102	0.22	4.210	No	19.55	18.63	126.769	0.137	0.477	0.861	4
103	0.15	3.224	No	17.87	44.24	187.922	0.147	0.859	1.057	4
104	0.19	4.607	No	28.08	25.91	242.122	0.154	0.655	1.037	4
105	0.14	3.627	No	19.59	38.52	189.474	0.161	1.000	1.188	4
106	0.14	3.840	No	23.76	40.69	131.075	0.162	0.965	1.189	4
107	0.21	5.852	No	20.12	32.79	236.744	0.166	0.628	1.103	4
108	0.19	5.427	No	24.74	45.11	179.936	0.167	0.708	1.140	4
109	0.19	5.922	No	32.10	33.48	299.505	0.175	0.743	1.202	4
110	0.19	6.130	No	36.27	28.65	425.259	0.179	0.777	1.244	4
111	0.18	5.760	Yes	21.43	38.96	162.497	0.179	0.839	1.266	4
112	0.16	5.415	No	17.90	33.88	207.870	0.181	0.938	1.313	4
113	0.17	5.993	No	21.30	29.88	134.942	0.185	0.879	1.314	4
114	0.18	6.717	No	21.68	51.59	123.726	0.194	0.905	1.385	4
115	0.23	10.458	No	32.24	27.06	816.588	0.212	0.707	1.427	4
116	0.15	8.700	No	29.51	43.15	161.755	0.240	1.375	1.869	4

Table A-2
Properties of the rocks and flow displacement experiments (Reservoir B).

Test ID	φ (fr.)	K (mD)	Crude aging	S_{wi} (%)	S_{or} (%)	DRQI (mD/cp)	RQI (μm)	FZI (μm)	r35 (μm)	GHE* no.
1	0.11	0.007	No	31.16	53.56	0.089	0.008	0.066	0.037	1
2	0.06	0.005	Yes	19.27	43.53	0.063	0.009	0.130	0.048	1
3	0.06	0.005	No	3.31	51.71	0.437	0.009	0.134	0.049	1
4	0.09	0.011	No	24.69	54.02	0.218	0.011	0.116	0.058	1
5	0.12	0.018	Yes	22.22	7.06	2.215	0.012	0.087	0.059	1
6	0.14	0.024	Yes	15.44	14.71	1.819	0.013	0.080	0.062	2
7	0.15	0.030	Yes	13.75	19.61	1.013	0.014	0.084	0.068	2
8	0.13	0.052	Yes	14.65	26.45	4.432	0.020	0.128	0.101	2
9	0.19	0.074	Yes	41.11	23.73	0.484	0.020	0.087	0.093	2
10	0.21	0.086	Yes	17.92	29.15	2.095	0.020	0.074	0.091	2
11	0.13	0.063	No	3.35	49.35	3.327	0.021	0.138	0.112	2
12	0.16	0.096	No	16.77	29.52	5.074	0.024	0.124	0.122	2
13	0.10	0.071	No	20.58	52.83	2.038	0.026	0.224	0.151	2

(*continued on next page*)

Table A-2 (*continued*)

Test ID	φ (fr.)	K (mD)	Crude aging	S_{wi} (%)	S_{or} (%)	DRQI (mD/cp)	RQI (μm)	FZI (μm)	r35 (μm)	GHE* no.
14	0.11	0.084	No	26.95	39.11	2.750	0.027	0.217	0.156	2
15	0.15	0.164	No	34.91	29.31	7.887	0.033	0.181	0.177	2
16	0.23	0.300	Yes	16.08	28.74	10.290	0.036	0.119	0.176	2
17	0.14	0.187	No	35.32	31.26	13.966	0.037	0.227	0.208	2
18	0.17	0.276	Yes	20.00	13.91	21.198	0.040	0.188	0.215	2
19	0.11	0.191	Yes	22.50	54.96	2.536	0.041	0.338	0.258	3
20	0.06	0.106	No	20.17	36.52	5.011	0.042	0.661	0.308	3
21	0.10	0.191	Yes	7.38	41.33	5.686	0.042	0.365	0.269	3
22	0.16	0.305	Yes	18.34	43.47	14.352	0.044	0.236	0.249	3
23	0.16	0.350	No	23.85	30.85	11.826	0.046	0.241	0.263	3
24	0.14	0.330	Yes	24.12	33.31	3.278	0.048	0.298	0.289	3
25	0.12	0.290	No	33.15	35.72	10.589	0.049	0.354	0.303	3
26	0.19	0.493	No	6.78	23.15	64.144	0.051	0.215	0.279	3
27	0.09	0.228	No	28.50	45.98	8.011	0.051	0.552	0.355	3
28	0.09	0.248	No	39.19	33.06	5.387	0.053	0.549	0.364	3
29	0.14	0.436	No	21.21	43.48	18.963	0.055	0.324	0.330	3
30	0.15	0.497	No	25.93	31.99	21.379	0.057	0.317	0.341	3
31	0.23	1.001	Yes	19.51	4.01	54.791	0.065	0.214	0.355	3
32	0.17	0.748	No	26.96	38.81	31.334	0.066	0.320	0.393	3
33	0.18	0.831	No	37.24	22.24	37.756	0.067	0.294	0.389	3
34	0.24	1.238	Yes	20.94	25.82	22.255	0.071	0.223	0.390	3
35	0.16	0.837	No	18.86	40.92	46.672	0.071	0.370	0.439	3
36	0.15	0.801	No	32.52	44.84	12.948	0.073	0.415	0.458	3
37	0.17	1.039	No	6.17	58.80	15.957	0.077	0.373	0.474	3
38	0.14	0.947	No	36.18	23.54	26.633	0.081	0.497	0.532	3
39	0.24	1.658	Yes	24.12	3.79	61.562	0.083	0.264	0.468	3
40	0.22	1.698	No	33.63	35.40	55.535	0.087	0.300	0.502	3
41	0.18	1.496	No	31.35	31.74	67.454	0.090	0.409	0.561	3
42	0.25	2.273	Yes	17.81	35.63	51.775	0.094	0.279	0.537	3
43	0.30	2.822	Yes	19.39	14.09	90.424	0.096	0.222	0.523	3
44	0.26	2.432	No	46.34	12.01	169.910	0.097	0.283	0.554	3
45	0.25	2.428	No	45.75	12.34	57.648	0.097	0.285	0.556	3
46	0.13	1.346	No	35.16	37.20	34.738	0.100	0.658	0.690	3
47	0.20	2.046	No	30.84	32.42	46.639	0.101	0.406	0.621	3
48	0.18	2.307	No	31.47	43.18	19.407	0.113	0.528	0.737	3
49	0.12	1.614	No	12.70	43.62	65.968	0.116	0.856	0.841	3
50	0.16	2.362	No	22.63	30.33	102.505	0.120	0.622	0.808	4
51	0.24	3.706	No	25.04	31.07	75.114	0.123	0.389	0.747	4
52	0.27	4.604	No	14.63	34.83	103.655	0.129	0.346	0.763	4
53	0.27	4.591	No	18.44	34.07	130.271	0.130	0.352	0.769	4
54	0.23	4.261	No	30.18	27.63	63.371	0.134	0.439	0.831	4
55	0.25	4.584	No	31.13	24.14	181.047	0.135	0.405	0.820	4
56	0.18	3.396	No	40.54	27.87	33.224	0.135	0.602	0.897	4
57	0.26	5.075	No	11.91	40.13	92.317	0.139	0.396	0.841	4
58	0.21	5.707	No	30.09	36.46	136.654	0.164	0.616	1.082	4
59	0.25	6.807	No	25.23	32.30	219.339	0.164	0.496	1.037	4
60	0.24	6.687	No	24.47	31.38	122.505	0.166	0.526	1.059	4
61	0.26	7.597	No	30.71	28.90	182.450	0.170	0.483	1.064	4
62	0.25	7.300	No	38.83	13.47	425.995	0.171	0.523	1.090	4
63	0.21	6.620	No	31.91	30.85	237.505	0.178	0.688	1.202	4
64	0.14	4.971	No	38.14	21.54	171.156	0.185	1.113	1.393	4
65	0.22	8.014	No	23.22	38.45	224.095	0.188	0.651	1.250	4
66	0.27	10.672	No	23.93	29.69	299.211	0.198	0.541	1.267	4
67	0.20	7.929	No	8.87	49.11	174.152	0.199	0.806	1.382	4
68	0.23	10.516	No	21.51	32.09	316.890	0.214	0.727	1.449	4
69	0.22	11.462	No	29.98	31.73	161.529	0.224	0.775	1.540	4
70	0.22	28.142	No	33.67	28.62	867.899	0.357	1.283	2.681	4

Table A-3
Properties of the rocks and flow displacement experiments (Reservoir C).

Test ID	φ (fr.)	K (mD)	Crude aging	S_{wi} (%)	S_{or} (%)	DRQI (mD/cp)	RQI (μm)	FZI (μm)	r35 (μm)	GHE* no.
1	0.12	0.003	Yes	57.67	13.20	0.010	0.005	0.035	0.020	1
2	0.07	0.007	No	24.28	51.95	0.441	0.010	0.146	0.057	1
3	0.07	0.008	Yes	6.76	9.25	0.406	0.011	0.155	0.062	1
4	0.07	0.014	No	5.63	55.06	0.870	0.014	0.205	0.086	2
5	0.09	0.025	Yes	19.80	13.14	0.367	0.017	0.181	0.096	2
6	0.09	0.030	Yes	21.57	22.18	0.147	0.019	0.200	0.108	2
7	0.09	0.036	Yes	9.58	14.63	2.190	0.019	0.185	0.109	2
8	0.09	0.046	No	8.94	31.61	2.316	0.023	0.247	0.138	2
9	0.08	0.046	No	10.15	42.51	5.850	0.023	0.261	0.143	2
10	0.09	0.053	No	16.01	28.92	6.637	0.025	0.266	0.151	2

(*continued on next page*)

Table A-3 (*continued*)

Test ID	φ (fr.)	K (mD)	Crude aging	S_{wi} (%)	S_{or} (%)	DRQI (mD/cp)	RQI (μm)	FZI (μm)	r35 (μm)	GHE* no.
11	0.09	0.055	Yes	36.25	36.55	0.193	0.025	0.256	0.149	2
12	0.09	0.065	No	22.27	13.44	11.272	0.026	0.248	0.155	2
13	0.11	0.097	No	7.41	31.79	12.409	0.030	0.253	0.178	2
14	0.09	0.084	No	14.89	40.74	2.180	0.031	0.332	0.197	2
15	0.06	0.063	No	11.63	37.02	9.723	0.031	0.467	0.216	2
16	0.12	0.147	No	11.81	32.87	9.807	0.036	0.273	0.212	2
17	0.10	0.154	Yes	26.23	30.53	0.737	0.038	0.329	0.237	2
18	0.09	0.145	No	16.67	42.01	5.911	0.040	0.397	0.257	2
19	0.11	0.182	Yes	15.09	9.28	5.228	0.040	0.317	0.246	3
20	0.11	0.179	Yes	12.09	27.91	4.241	0.041	0.337	0.252	3
21	0.09	0.147	No	21.05	25.31	16.890	0.041	0.445	0.275	3
22	0.13	0.234	Yes	47.81	12.86	11.330	0.043	0.292	0.255	3
23	0.13	0.261	Yes	41.68	18.27	1.891	0.045	0.301	0.268	3
24	0.10	0.233	No	11.02	33.22	21.636	0.047	0.416	0.307	3
25	0.09	0.207	No	22.45	36.37	7.348	0.048	0.496	0.325	3
26	0.11	0.280	No	18.51	33.43	24.255	0.050	0.393	0.316	3
27	0.10	0.284	No	15.60	17.98	38.439	0.052	0.447	0.340	3
28	0.09	0.322	No	22.27	30.47	25.308	0.058	0.554	0.398	3
29	0.15	0.546	Yes	16.90	20.27	8.986	0.060	0.340	0.364	3
30	0.09	0.332	Yes	33.93	15.53	3.903	0.060	0.609	0.422	3
31	0.11	0.486	Yes	17.74	28.02	13.710	0.066	0.536	0.445	3
32	0.09	0.639	No	12.28	33.05	62.684	0.084	0.844	0.621	3
33	0.11	0.780	No	17.00	56.35	34.513	0.084	0.679	0.588	3
34	0.15	1.410	No	10.81	33.18	33.833	0.096	0.546	0.637	3

References

Abbasi, J., Riazi, M., Ghaedi, M., Mirzaei-Paiaman, A., 2017. Modified shape factor incorporating gravity effects for scaling countercurrent imbibition. J. Pet. Sci. Eng. 150, 108–114.

Abdulaziz, A.M., Mahdi, H.A., Sayyouh, M.H., 2019. Prediction of reservoir quality using well logs and seismic attributes analysis with an artificial neural network: a case study from Farrud Reservoir, Al-Ghani Field, Libya. J. Appl. Geophys. 161, 239–254.

Abuamarah, B.A., Nabawy, B.S., 2021. A proposed classification for the reservoir quality assessment of hydrocarbon-bearing sandstone and carbonate reservoirs: a correlative study based on different assessment petrophysical procedures. J. Nat. Gas Sci. Eng. 88, 103807.

Aguilera, R., 2002. Incorporating capillary pressure, pore throat aperture radii, height above free-water table, and Winland r35 values on Pickett plots. AAPG Bull. 86 (4), 605–624.

Akin, S., Schembre, J.M., Bhat, S.K., Kovscek, A.R., 2000. Spontaneous imbibition characteristics of diatomite. J. Pet. Sci. Eng. 25, 149–165.

Amaefule, J.O., Altunbay, M., Tiab, D., Kersey, D.G., Keelan, D.K., 1993. Enhanced reservoir description using core and log data to identify hydraulic flow units and predict permeability in uncored intervals/wells. In: SPE Annual Technical Conference and Exhibition, 3–6 October, Houston, Texas.

American Petroleum Institute, February 1998. Recommended Practices for Core Analysis. Recommended Practice, p. 40.

Armstrong, R.T., Sun, C., Mostaghimi, P., Berg, S., Rucker, M., Luckham, P., Georgiadis, A., McClure, J., 2021. Multiscale characterization of wettability in porous media. Transport Porous Media 140, 215–240.

Babu, D., Odeh, A.S., 1989. Productivity of a horizontal well. SPE Reservoir Eng. 4 (4), 417–421.

Blackbourn, G.A., 2012. Cores and Core Logging for Geoscientists. Whittles, Dunbeath.

Blunt, M.J., 2017. Multiphase Flow in Permeable Media. A Pore-Scale Perspective. Cambridge University Press.

Brown, H.W., 1951. Capillary pressure investigations. Petroleum Transactions, AIME 192, 67–74.

Cai, J., Perfect, E., Cheng, C., Hu, X., 2014. Generalized modeling of spontaneous imbibition based on Hagen−Poiseuille flow in tortuous capillaries with variably shaped apertures. Langmuir 30, 5142–5151.

Chandra, V., Barnett, A., Corbett, P., Geiger, S., Wright, P., Steele, R., Milroy, P., 2015. Effective integration of reservoir rock-typing and simulation using near-wellbore upscaling. Mar. Petrol. Geol. 67, 307–326.

Chopra, A.K., 1988. Reservoir descriptions via pulse testing: a technology evaluation. In: SPE-17568-MS, International Meeting on Petroleum Engineering, 1–4 November, Tianjin, China.

Chopra, A.K., Stein, M.H., Ader, J.C., 1989. Development of reservoir descriptions to aid in design of EOR projects. SPE-16370-PA. SPE Reservoir Eng. 4 (2), 143–150.

Corbett, P., Potter, D.K., 2004. Petrotyping: a basemap and atlas for navigating through permeability and porosity data for reservoir comparison and permeability prediction. In: Paper SCA2004-30, International Symposium of the Society of Core Analysts Held in Abu Dhabi, UAE, 5-9 October 2004.

Cullick, A.S., Narayanan, K., Gorell, S.B., 2005. Optimal field development planning of well locations with reservoir uncertainty. In: Paper Presented at the SPE Annual Technical Conference and Exhibition, Dallas, Texas, October 2005. https://doi.org/10.2118/96986-MS. Paper Number: SPE-96986-MS.

da Cruz, P.S., Horne, R.N., Deutsch, C.V., 2004. The quality map: a tool for reservoir uncertainty quantification and decision making. SPE Reservoir Eval. Eng. 7 (1), 6–14.

Ding, S., Jiang, H., Li, J., Tang, G., 2014. Optimization of well placement by combination of a modified particle swarm optimization algorithm and quality map method. Comput. Geosci. 18 (5), 747–762.

Dullien, F.A.L., 1992. Porous Media: Fluid Transport and Pore Structure, second ed. Academic Press, San Diego.

Faramarzi-Palangar, M., Mirzaei-Paiaman, A., 2021. Investigating dynamic rock quality in two-phase flow systems using TEM-function: a comparative study of different rock typing indices. Petroleum Research 6 (1), 16–25. https://doi.org/10.1016/j.ptlrs.2020.08.001.

Ghanbarian, B., Lake, L.W., Sahimi, M., 2019. Insights into rock typing: a critical study. SPE J. 24 (1), 230–242.

Ghedan, S.G., 2007. Dynamic rock types for generating reliable and consistent saturation functions for simulation models. In: SPE/EAGE Reservoir Characterization and Simulation Conference, Abu Dhabi, UAE, 28–31 October.

Gluyas, J., Swarbrick, R., 2004. Petroleum Geoscience. Blackwell, Oxford.

Gomes, J.S., Ribeiro, M.T., Strohmenger, C.J., Negahban, S., Kalam, M.Z., 2008. Carbonate reservoir rock typing-the link between geology and SCAL. In: SPE-118284-MS, Abu Dhabi International Petroleum Exhibition and Conference, 3-6 November, Abu Dhabi, UAE.

Hamidpour, E., Fathollahi, S., Mirzaei-Paiaman, A., Bardestani, M., Kamalifar, H., 2018. The study of spontaneous Co-current and counter-current imbibition in heavy oil fractured reservoirs with the focus on their distinctions in numerical simulation methods. In: Paper Presented at the SPE International Heavy Oil Conference and Exhibition, Kuwait City, Kuwait, December 2018. https://doi.org/10.2118/193767-MS. Paper Number: SPE-193767-MS.

Hamidpour, E., Mirzaei-Paiaman, A., Masihi, M., Harimi, B., 2015. Experimental study of some important factors on nonwetting phase recovery by cocurrent spontaneous imbibition. J. Nat. Gas Sci. Eng. 27 (Part 2), 1213–1228. https://doi.org/10.1016/j.jngse.2015.09.070.

Hamon, G., Bennes, M., 2004. Two-phase flow rock typing: another approach. Petrophysics 45 (5), 433–444.

Handy, L.L., 1960. Determination of effective capillary pressure for porous media from imbibition data. Pet. Trans. AIME 219, 75–80.

Harimi, B., Masihi, M., Mirzaei-Paiaman, A., Hamidpour, E., 2019. Experimental study of dynamic imbibition during water flooding of naturally fractured reservoirs. J. Pet. Sci. Eng. 174, 1–13.

Hu, Q.H., Ewing, R.P., 2014. Integrated Experimental and Modeling Approaches to Studying the Fracture-Matrix Interaction in Gas Recovery from Barnett Shale. University of Texas at Arlington (Prepared for US Department of Energy). Report 09122-12.

Jadhunandan, P.P., Morrow, N.R., 1995. Effect of wettability on waterflood recovery for crude-oil/brine/rock systems. SPE Reservoir Eng. 10 (1), 40–46.

Jaya, I., Sudaryanto, A., Widarsono, B., 2005. Permeability prediction using pore throat and rock fabric: a model from Indonesian reservoirs. In: SPE-93363-MS, SPE Asia Pacific Oil and Gas Conference and Exhibition, 5–7 April, Jakarta, Indonesia. https://doi.org/10.2118/93363-MS.

Jones, S.C., 1978. Graphical techniques for determining relative permeability from displacement experiments. J. Petrol. Technol. 30, 807–81705.

Kolodzie, S., 1980. Analysis of pore throat size and use of the Waxman-Smits equation to determine OOIP in Spindle field. In: Colorado. SPE-9382-MS, SPE Annual Technical Conference and Exhibition, 21–24 September, Dallas, Texas. https://doi.org/10.2118/9382-MS.

Leverett, M.C., 1941. Capillary behaviour in porous solids. Transactions of the AIME 142, 159–172.

Liu, H., 2017. Fluid Flow in the Subsurface. Springer. https://link.springer.com/book/10.1007/978-3-319-43449-0.

Liu, H.H., Lai, B.T., Chen, J.H., 2015. Unconventional spontaneous imbibition into shale matrix: theory and a methodology to determine relevant parameters. Transport Porous Media. https://doi.org/10.1007/s11242-015-0580-z.

Liu, K., Mirzaei-Paiaman, A., Liu, B., Ostadhassan, M., 2020. A new model to estimate permeability using mercury injection capillary pressure data: application to carbonate and shale samples. J. Nat. Gas Sci. Eng. 84, 103691.

Liu, N., Jalali, Y., 2006. Closing the loop between reservoir modeling and well placement and positioning. In: Paper Presented at the Intelligent Energy Conference and Exhibition, Amsterdam, The Netherlands, April 2006. https://doi.org/10.2118/98198-MS. Paper Number: SPE-98198-MS.

Martini, R., Schiozer, D., Nakajima, L., 2005. Use of quality maps in reservoir management. J. Braz. Soc. Mech. Sci. Eng. 27 (4), 463–468.

Masalmeh, S.K., Jing, X.D., 2004. Carbonate SCAL: characterisation of carbonate rock types for determination of saturation functions and residual oil saturations. In: Paper SCA2004-08, International Symposium of the Society of Core Analysts Held in Abu Dhabi, UAE, 5-9 October.

Maschio, C., Nakajima, L., Schiozer, D.J., 2008. Production strategy optimization using genetic algorithm and quality map. In: Paper Presented at the Europec/EAGE Conference and Exhibition, Rome, Italy, June 2008. https://doi.org/10.2118/113483-MS. Paper Number: SPE-113483-MS.

McPhee, C., Reed, J., Zubizarreta, I., 2015. In: Core Analysis: A Best Practice Guide, first ed., ume 64. Elsevier, eBook, ISBN 9780444636577. Hardcover 9780444635334.

Min, B., Park, C., Kang, J., Park, H., Jang, I., 2011. Optimal well placement based on artificial neural network incorporating the productivity potential. Energy Sources, Part A Recovery, Util. Environ. Eff. 33 (18), 1726–1738.

Mirzaei-Paiaman, A., Ghanbarian, B., 2021b. A note on dynamic rock typing and TEM-function for grouping, averaging and assigning relative permeability data to reservoir simulation models. J. Nat. Gas Sci. Eng. 87, 103789.

Mirzaei-Paiaman, A., Ghanbarian, B., 2021a. A new methodology for grouping and averaging capillary pressure curves for reservoir models. Energy Geoscience 2 (1), 52–62. https://doi.org/10.1016/j.engeos.2020.09.001.

Mirzaei-Paiaman, A., Asadolahpour, S.R., Saboorian-Jooybari, H., Chen, Z., Ostadhassan, M., 2020. A new framework for selection of representative samples for special core analysis. Petroleum Research 5 (3), 210–226. https://doi.org/10.1016/j.ptlrs.2020.06.003.

Mirzaei-Paiaman, A., Ostadhassan, M., Rezaee, R., Saboorian-Jooybari, H., Chen, Z., 2018. A new approach in petrophysical rock typing. J. Petrol. Sci. Eng. 166, 445–464.

Mirzaei-Paiaman, A., Sabbagh, F., Ostadhassan, M., Shafiei, A., Rezaee, R., Saboorian-Jooybari, H., Chen, Z., 2019a. A further verification of FZI* and PSRTI: newly developed petrophysical rock typing indices. J. Petrol. Sci. Eng. 175, 693–705.

Mirzaei-Paiaman, A., Saboorian-Jooybari, H., 2016. A method based on spontaneous imbibition for characterization of pore structure: application in pre-SCAL sample selection and rock typing. J. Nat. Gas Sci. Eng. 35, 814–825. https://doi.org/10.1016/j.jngse.2016.09.023.

Mirzaei-Paiaman, A., Saboorian-Jooybari, H., Chen, Z., Ostadhassan, M., 2019b. New technique of True Effective Mobility (TEM-Function) in dynamic rock typing: reduction of uncertainties in relative permeability data for reservoir simulation. J. Petrol. Sci. Eng. 179, 210–227.

Mirzaei-Paiaman, A., Saboorian-Jooybari, H., Pourafshari, P., 2015. Improved method to identify hydraulic flow units for reservoir characterization. Energy Technol. 3 (7), 726–733.

Nabawy, B.S., 2013. Impacts of dolomitization on the petrophysical properties of el-halal formation, north sinai, Egypt. Arabian J. Geosci. 6, 359–373.

Nabawy, B.S., El Sharawy, M.S., 2018. Reservoir assessment and quality discrimination of Kareem Formation using integrated petrophysical data. Southern Gulf of Suez, Egypt, Marine and Petroleum Geology 93, 230–246.

Nakajima, L., Schiozer, D.J., 2003. Horizontal well placement optimization using quality map definition. In: Paper Presented at the Petroleum Society's Canadian International Petroleum Conference 2003, Calgary, Alberta, Canada, June 10 – 12.

Narayanasamy, R., Davies, D.R., Somerville, J.M., 2006. Well location selection from a static model and multiple realisations of a geomodel using productivity potential map technique. In: Paper Presented at the SPE Europec/EAGE Annual Conference and Exhibition, Vienna, Austria, June 2006. https://doi.org/10.2118/99877-MS. Paper Number: SPE-99877-MS.

Nazari, M.H., Tavakoli, V., Rahimpour-Bonab, H., Sharifi-Yazdi, M., 2019. Investigation of factors influencing geological heterogeneity in tight gas carbonates, Permian reservoir of the Persian Gulf. J. Petrol. Sci. Eng. 183, 106341.

Ngo, V.T., Lu, V.D., Nguyen, M.H., Hoang, T.M., Nguyen, H.M., Le, V.M., 2015. A Comparison of permeability prediction methods using core analysis data. In: SPE−175650−MS, SPE Reservoir Characterisation and Simulation Conference and Exhibition, 14−16 September, Abu Dhabi, UAE.

Oliveira, G.P., Santos, M.D., Roemers-Oliveira, E., 2021. Well placement subclustering within partially oil-saturated flow units. J. Petrol. Sci. Eng. 196, 107730.

Ozkan, A., Cumella, S.P., Milliken, K.L., Laubach, S.E., 2011. Prediction of lithofacies and reservoir quality using well logs, late cretaceous williams fork formation, mamm creek field, piceance basin, Colorado. AAPG (Am. Assoc. Pet. Geol.) Bull. 95 (10), 1699–1723.

Pittman, E.D., 1992. Relationship of porosity and permeability to various parameters derived from mercury injection-capillary pressure curves for sandstone. AAPG Bull. 76, 191–198.

Pouladi, B., Karkevandi-Talkhooncheh, A., Sharifi, M., Gerami, S., Nourmohammad, A., Vahidi, A., 2020. Enhancement of spsa algorithm performance using reservoir quality maps: application to coupled well placement and control optimization problems. J. Petrol. Sci. Eng. 189.

Purcell, W.R., 1949. Capillary pressures-their measurement using mercury and the calculation of permeability therefrom. Am. Inst. Mech. Eng. Petroleum Transaction, AIME, T.P 2544, 39–48.

Ravalec, M.L., 2012. Optimizing well placement with quality maps derived from multi-fidelity meta-models. In: Paper Presented at the SPE Europec/EAGE Annual Conference, Copenhagen, Denmark. https://doi.org/10.2118/154416-MS. Paper Number: SPE-154416-MS.

Roychaudhuri, R., Tsotsis, T.T., Jessen, K., 2013. An experimental investigation of spontaneous imbibition in gas shales. J. Petrol. Sci. Eng. 111, 87–97.

Skalinski, M., Jeroen, A., Kenter, M., 2014. Carbonate Petrophysical Rock Typing: Integrating Geological Attributes and Petrophysical Properties while Linking with Dynamic Behavior. Geological Society, London, Special Publications, first published May 30. https://doi.org/10.1144/SP406.6.

Skauge, A., Ottesen, B., 2002. A summary of experimentally derived relative permeability and residual saturation on North Sea reservoir cores. In: Paper SCA2002-12. International Symposium of the Society of Core Analysts (SCA), Monterey, California, USA.

Swanson, B.F., 1981. Simple correlation between permeabilities and mercury capillary pressures. J. Petrol. Technol. 2498–2504.

Tavakoli, V., 2018. Geological Core Analysis, Application to Reservoir Characterization. Springer, SpringerBriefs in Petroleum Geoscience & Engineering. https://doi.org/10.1007/978-3-319-78027-6.

Tavakoli, V., 2021. Permeability's response to dolomitization, clues from Permian–Triassic reservoirs of the central Persian Gulf. Mar. Petrol. Geol. 123, 104723.

Thomeer, J.H.M., 1960. Introduction of a pore geometrical factor defined by the capillary pressure curve. SPE-1324-G J. Pet. Technol. 12 (3), 73–77. https://doi.org/10.2118/1324-G.

Tran, H., Kasha, A., Sakhaee-Pour, A., Hussein, I., 2020. Predicting carbonate formation permeability using machine learning. J. Petrol. Sci. Eng. 195, 107581.

Worden, R.H., Armitage, P.J., Butcher, A.R., Churchill, J.M., Csoma, A.E., Hollis, C., Lander, R.H., Omma, J.E., 2018. Petroleum reservoir quality prediction: overview and contrasting approaches from sandstone and carbonate communities. Geological Society, London, Special Publications 435, 1–31.

Yokeley, B.A., Ghanbarian, B., Sahimi, M., 2021. Rock typing based on wetting-phase relative permeability data and critical pore sizes. SPE J. 26 (6), 3893–3907.

Zhao, X., Blunt, M.J., Yao, J., 2010. Pore-scale modeling: effects of wettability on waterflood oil recovery. J. Petrol. Sci. Eng. 71, 169–178.